# Enhanced net $CO_2$ exchange of a semi-deciduous forest in the southern Amazon due to diffuse radiation from biomass burning

Simone Rodrigues[1,*], Glauber Cirino[1,3,4,*], Demerval Moreira[2], Rafael Palácios[3,4], José Nogueira[†], Maria Isabel Vitorino[1,3], and George Vourlitis[5,*]

[1]Programa de Pós-Graduação em Ciências Ambientais, Universidade Federal do Pará, Belém-PA, Brazil
[2]Faculdade de Ciências, Universidade Estadual Paulista, Bauru-SP, Brazil
[3]Instituto de Geociências, Faculdade de Meteorologia, Universidade Federal do Pará, Belém-PA, Brazil
[4]Programa de Pós-Graduação em Gestão de Risco e Desastre na Amazônia, Universidade Federal do Pará, Belém-PA, Brazil
[5]Department of Biological Sciences, California State University, San Marcos, CA, USA
[*]These authors contributed equally to this work
[†]Deceased

**Correspondence:** G. Vourlitis (georgev@csusm.edu)

**Abstract.** Atmospheric processes and climate are closely linked to the carbon cycle in the Amazon region as a consequence of the strong biosphere-atmosphere coupling. The radiative effects of aerosols and clouds are still unknown for a wide variety of species and types of vegetation present in Amazonian biomes. This study examines the effects of atmospheric aerosols on solar radiation and their effects on Net Ecosystem Exchange (NEE) in an area of semideciduous tropical forest in the North of Mato Grosso State. Our results show a reduction in the NEE with a decrease in incident solar radiation of $\approx 40\%$ and relative irradiance between 1.10-0.67. However, an average increase of 35-70% in NEE was observed when pollution levels (Aerosol Optical Depth) were above $\approx 1.25$. The increase NEE was attributed to the increase of up to 60% in the diffuse fraction of Photosynthetically Active Radiation. These results were mainly attributable to the biomass burning organic aerosols from fires. Important influences on temperature and relative humidity of the air, induced by the interaction between solar radiation and high aerosol load in the observation area, were also noticed; an average cooling of $\approx 3.0°C$ and 10%, respectively. Given the long-distance transport of aerosols emitted by burning biomass, significant changes in $CO_2$ flux can occur over large areas of the Amazon, with important effects on the potential for $CO_2$ absorption on ecosystems of semideciduous forests distributed in the region.

## 1   Introduction

Carbon (C) is a key element in global biogeochemical cycles, and understanding the biosphere-atmosphere fluxes of mass and energy is essential to understanding current and future terrestrial C storage. In the context of global climate change, the potential for terrestrial ecosystems to modulate increases in anthropogenic $CO_2$ emissions, through the process of net ecosystems $CO_2$ exchnage (NEE), has been widely debated Booth et al. (2012); Huntingford et al. (2013); Brienen et al. (2015), especially for Amazonian tropical forests Doughty et al. (2015); Braghiere, Kerches Renato, Akemi Yamasoe et al. (2020); Gatti et al. (2014, 2021). The result of increasing atmospheric $CO_2$ levels provides important feedback on the future of

greenhouse warming Booth et al. (2012); Huntingford et al. (2013). In the Amazon biome, forest ecosystems play an important role in terrestrial C storage, and while these forests seem to have a uniform behavior, there are distinct climatic sub-regions that affect C storage Brienen et al. (2015); Gatti et al. (2021). $CO_2$ absorption through photosyn-thesis increases the vegetation and soil C stocks, representing a C sink, while plant, animal, and microbial respiration release $CO_2$ into the atmosphere,

25 representing a C source to the atmosphere. Photosynthesis and respiration processes can vary considerably from subregion to sub-region in Amazonia, resulting in distinct carbon source or sink behaviors depending on geographic location and climatic conditions Doughty et al. (2015); Silva et al. (2020).

In general, the participation of forests in the global carbon cycle can only be adequately quantified by long-term studies monitoring C exchange at the plant-atmosphere interface. Forests are estimated to store 200-300 Pg C Pan (2011); Saatchi

30 et al. (2011); Avitabile et al. (2016), about a third of what is contained in the atmosphere. This stock is very dynamic, and these trees process about 60% of global photosynthesis, sequestering about 72 Pg C from the atmospheric component through gross primary production (GPP) every year Beer et al. (2010) but releasing a similar amount back into the atmosphere from ecosystem (plant +animal+microbial) respiration Nagy et al. (2018). With these large fluxes, a small proportionate change in $CO_2$ uptake or release can result in a large net C source or sink.

35 Carbon concentrations in the atmosphere have increased since the beginning of the industrial period and currently act with other C emission sources, such as the degradation of forests, mainly tropical ones. Recent reports Gatti et al. (2021) show that some regions of the Amazon act as a source of $CO_2$ to the atmosphere, as a result of logging, land use change, and fires that occur in the region. However, other research indicates that Amazonian forests may be net sinks of atmospheric $CO_2$ Carswell et al. (2002); von Randow et al. (2004) or approximately in equilibrium Vourlitis et al. (2011). In general, the balance between

40 rates of carbon emission or carbon fixation is delicate, so small external disturbances can change the dynamics of the forest and the state of the climate system.

Among the modulating agents of the $CO_2$ balance, solar radiation is a fundamental component for both photosynthesis and respiration. In Brazil, and especially in the Amazon region, the burning of biomass emits large amounts of gases and aerosols into the atmosphere, these emissions can strongly alter radiative fluxes, impacting $CO_2$ Aragão et al. (2018); Malavelle et al.

45 (2019); Morgan et al. (2019); de Magalhães et al. (2019). Atmospheric aerosols from biomass burning affect ecosystem light use efficiency ($LUE$) and productivity, influence the amount and nature of solar radiation received in the system, and affect other environmental conditions such as temperature and humidity Kanniah et al. (2012); Mercado et al. (2009). Studies of the effects of aerosols on terrestrial C cycling processes have found positive, negative, and neutral effects, and most of the research in the Amazon have been conducted in the central Cirino et al. (2014), eastern Doughty et al. (2010); Oliveira et al. (2007), and

50 southwestern Yamasoe et al. (2006); Cirino et al. (2014) parts of the basin. However, litter research has been done in seasonal forests, which lie within the "arc of deforestation" and the ecotone between Amazonian Forest and Cerrado, and other key tropical ecosystems such as Pantanal forests and Cerrado forests and woodlands. Modeling studies have also demonstrated the impact of aerosols on GPP on a regional Moreira et al. (2013); Bian et al. (2021) and global Mercado et al. (2009); Rap (2015) scale.

55    The models, however, need improvements in the parameterization of the radiative effects of aerosols and clouds. These improvements are fundamental for more accurate and realistic specialization of the potential for the absorption of atmospheric $CO_2$ by the Amazon as a whole Aragão et al. (2018). In this sense, the potential for fire induced atmospheric aerosols to impact to $CO_2$ absorption by tropical semideciduous (seasonal) forests in Mato Grosso (in the arc of deforestation) has not been evaluated either by direct observation or numerical modeling. It is known that these forests play a central role in preserving

60    biodiversity Fu et al. (2018), are located on the frontier of deforestation, and experience seasonal variations in NEE Vourlitis et al. (2011). These attributes make this region an excellent laboratory to assess the effects of atmospheric aerosols on forest NEE.

This research focuses on studying the action of biomass burning aerosols in an area of semi-deciduous forest located in the southern portion of the Amazon Basin, in the north of the State of Mato Grosso, in the region the arc of deforestation. To this

65    end, we specifically seek to: (1) develop a clear-sky irradiance algorithm using a long observation period of aerosol optical depth (AOD); (2) quantify the in-crease in the diffuse fraction of solar radiation due to the presence of aerosols from fires in the experimental study area; (3) quantify net and relative changes in $NEE$ from changes in direct and diffuse radiation; (4) to evaluate the influence of fires on biophysical variables that influence forest photosynthetic rates, such as leaf canopy temperature ($CL_T$, air temperature $T_{air}$, and the vapor pressure deficit (VPD). Aerosol data and micrometeorological measurements with

70    carbon fluxes measured by the eddy covariance system are used in the period 2005-2009. All solar radiation measurements are evaluated in terms of aerosol depth (AOD), solar zenith angle ($SZA$), and relative irradiance ($f$).

## 2 Materials and Methods

### 2.1 Site descriptions

The study area was located in the south of the Amazon basin, 50 km northeast of Sinop, in the municipality of Cláudia (Lat

75    11° 24.75' S, Long. 55° 19.50' W), in the State of Mato Grosso (Fig. 1). This forest is located in the arc of deforestation, a region of 105 continuous agricultural expansion, logging, and fires; Nepstad et al. (2014); Balch et al. (2015); Alencar et al. (2022) (Figs. S1, S2, and S3), and is recognized as seasonal, dry, or semideciduous forest Ackerly et al. (1989); Ratter et al. (1978). Supplementary Figs. S3 and S5 show the study area under different aerosol loads during the dry and rainy seasons, respectively. These figures were obtained from the time series of the Terra and Acqua Satellites ($AOD_m$, Table1).

80    Previous studies report the characteristics of this type of forest Vourlitis et al. (2011), which typically have trees with lower height, biomass, and floristic diversity compared to humid tropical forests Murphy and Lugo (1986); Nogueira et al. (2008) due to their well-defined seasonal variation in precipitation. The forest is 423 m above sea level, in a transition where the vegetation consists of Savannah (Cerrado), transitional vegetation (Cerradão), and Amazonian forest Vourlitis et al. (2011).

The deciduous and semi-deciduous forests within the Cerrado domain, initially covered over 49.95 km$^2$ in the state of Mato

85    Grosso, but currently, 20.50 km$^2$ of this area is deforested ($\approx 41\%$), and only 14% is located within protected areas Alencar et al. (2022). The geographic positions of these forests are discontinuous, due to climatic fluctuations that have occurred in the last 10,000 years Prado and Gibbs (1993). The tree species at this location are typical of the semi-deciduous forest of the
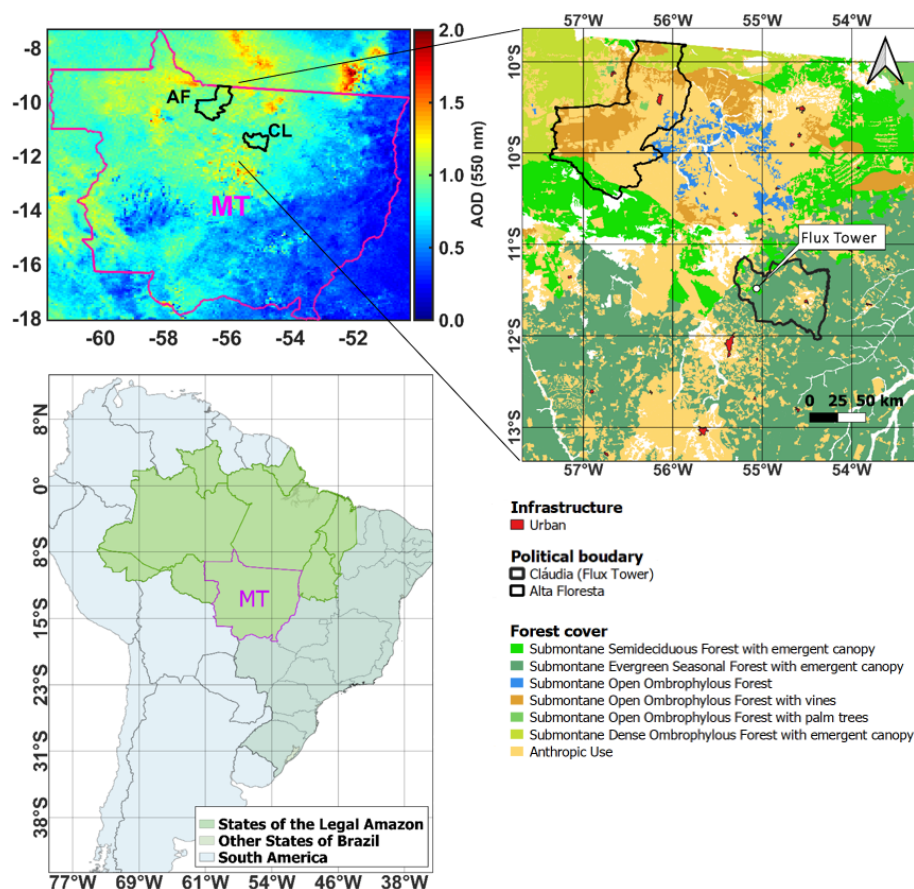
**Figure 1.** Localization map of a micrometeorological tower in the Cláudia municipality, 50 km northeast of Sinop, Mato Grosso (white point, in the right pane).

Amazon, with maximum canopy heights varying between 25-28 m. A comprehensive description of the species reported in the region was reported by Ackerly et al. (1989), Lorenzi (2000), and Lorenzi (2002). The soils are acidic with a pH measuring 4.2

90   and sandy (94% sand), well-drained quartzarenic neosols, poor in nutrients, and with low organic matter Vourlitis et al. (2001); Oliveira-Filho AT and Oliveira (2002), with a dry season that extends from May to September Vourlitis et al. (2002).

The 30-year average annual temperature in this area is 24 °C, with precipitation of approximately 2000 mm/year Vourlitis et al. (2002). Among the active atmospheric systems are the Bolivian High (BH), South Atlantic Convergence Zone (SACZ), and frontal Systems. To the north, the region is influenced by systems that operate in the Amazon, and the southern portion is

95   affected by extratropical systems, such as frontal systems Amorim Neto et al. (2015); Saraiva et al. (2016). The loss of leaves (deciduousness) during the dry season (July-September) is quite sensitive to water availability and temperatures (maximum and minimum) in the region. With the arrival of the rainy season (November-May), the vegetation recovers again with typical characteristics of tropical forests Vourlitis et al. (2011).

## 2.2 Instrumentation and Data

100    ### 2.2.1 Aerosol Measurements

This study used a long series of aerosol optical depth measurements – AOD (Aerosol Optical Depth) to assess the impact of atmospheric particles on the flux of solar radiation to the surface. Two types of remote sensors were used: the MODIS (Moderate Resolution Imaging Spectroradiometer) orbital sensor, available on board the AQUA and TERRA satellites, products MOD04-3K and MYD04-3K Remer et al. (2013), and an AERONET (Aerosol Robotic Network) solar photometer, used as

105 a standard measure of optical properties of atmospheric aerosols at the surface, between June1993-March2018 Holben et al. (1998). All remote aerosol information required for this study was operated and maintained by NASA (National Aeronautics and Space Administration).

The TERRA /AQUA satellites have a heliosynchronous polar orbit, with a Local Time (LT) of passage over the study areas around 10h30min and 13h30min. These space platforms cover the Earth's surface every 1-2 days with radiance measurements

110 in 36 spectral bands. The MOD/MYD043K aerosol products also feature the most current collection of data available from NASA, currently at 3 Km spatial resolution for AOD and other aerosol optical properties Levy et al. (2013); Remer et al. (2013). Filters to exclude contamination of data by clouds are also applied during estimation processing. The AOD series from these satellites has 20 years of data on continents and oceans and is widely available on the open access platform of the Atmospheric Files Distribution System – Level 1, located at the Distributed Active Files Center (LAADS-DAAC) from

115 Goddard Space Flight Center – GSFC, in Greenbelt, Maryland (USA). In this work, satellite AOD spatializations were used to obtain regional information on the nature or type of aerosol acting over the study area, between 2002-2020 (Fig. S4). More detailed information about the MODIS sensor, such as spectral models, validation, and operating period of the aforementioned products can be found in Remer et al. (2005, 2013).

A long series of AOD measurements (> 20 years of data) are available for the city of Alta Floresta in northern Mato

120 Grosso through CIMEL Electronique so-lar photometers, maintained and operated by NASA (GSFC), through the AERONET network (1993-2021). This photometer network is intended for the monitoring and characterization of aerosol particles in various regions of the world. These sensors represent the standard measure of AOD and are widely used in the validation of satellite AOD estimates. The system operates solar radiation measurements and rotational interference filters to extract optical properties from aerosols in various spectral bands, between 340-1020 nm Schafer et al. (2002b, a); Procopio et al. (2004);

125 Schafer et al. (2008). This makes it possible to evaluate the direct influence of atmospheric particles in real time on regions highly affected by fires, such as the region of the arc of deforestation. In this work, AOD was used at wavelengths of 500 nm (AERONET) and 550 nm (MODIS). Both satellite and photometer data cover the entire period of micrometeorological and flux data, described in the next section. In the Alta Floresta, the AERONET system also has individual sensors and long-term measurements of incident shortwave solar radiation ($SW_{ia}$), as described in Table 1.

**Table 1.** List of measured variables and instrumentation used in the micrometeorological tower (at Cláudia Municipality) and AERONET station, in Alta Floresta. The *flags* [1], [2] and [3] indicate the instrumentation used in the flux tower, AERONET system and AQUA space platforms (TERRA), respectively.

| Data set | | Instrumentation | | Attributes | |
|---|---|---|---|---|---|
| **Measurements** | **Sensors [sites]** | **Models, Manuf.** | **Units** | **Symbols** | **Height** |
| Inc. Solar Radiation | Pyranometer [1] | LI-200SB, LI-COR | $Wm^{-2}$ | $SW_i$ | 40.0 m |
| Photosyn. Active Rad. | Pyranometer [1] | LI-190SB, LI-COR | $Wm^{-2}$ | $PAR_i$ | 41.5 m |
| Atmospheric Pressure | Barometer [1] | PTB101B, VSLA | hPa | $P_{air}$ | 42.5 m |
| Air Temperature | Thermohygrometer [1] | CS215, RMS | °C | $T_{air}$ | 41.5 m |
| Relative Humidity | Thermohygrometer [1] | HMP-35, VSLA | % | $RH_{air}$ | 41.5 m |
| Precipitation | Pluviometer [1] | GAUGE, MANUAL | mm | PRP | 40.5 m |
| Wind Speed | Sonic Anemometer [1] | CSAT-3, CSCI | $ms^{-1}$ | $US_s$ | 42.0 m |
| Wind Direction | Sonic Anemometer [1] | CSAT-3, CSCI | deg | $US_d$ | 42.0 m |
| $CO_2$ Flux | Eddy system [1] | LI-COR | $\mu mol\, m^{-2}s^{-1}$ | $[FCO_2]$ | top |
| $CO_2$ Vertical Profile | IRGA [1] | LI-820, LI-COR | ppm | $[CO_2]$ | 1-28 m |
| Inc. Solar Radiation | Pyranometer [2] | CM21, K&Z | $Wm^{-2}$ | $SW_{ia}$ | – |
| Photosyn. Active Rad. | PAR Energy [2] | SKYE510, SKYE | $Wm^{-2}$ | $PAR_{ia}$ | – |
| Aerosol Optical Depth | Photometer [2] | CIMEL | - | $AOD_a$ | – |
| Aerosol Optical Depth | Modis-Terra [3] | MOD043K | - | $AOD_m$ | – |
| Aerosol Optical Depth | Modis-Aqua [3] | MYD043K | - | $AOD_m$ | – |

## 2.2.2 Micrometeorological Measurements

The $CO_2$ flux data set available for this research were widely used and cited by previous studies. Information regarding the systems installed in the micrometeorological tower is directly available in Vourlitis et al. (2011). An automatic weather station (ASW) to monitor the weather in the Cláudia municipality was used between Jun2005 and Jul2008. The implanted tower follows the standard of the micrometeorological measurement tower system of the Programa LBA Nagy et al. (2016); Artaxo et al. (2022). In this research, the deployed tower consists of a pyranometer, thermometer, psychrometer, anemometer, pluviograph, and a turbulent vortex system (*eddy covariance*). Herein, these measures were used to represent the biophysical factors that affect the photosynthetic rates of forests. Micrometeorological data were measured every 30-60 s and stored by data-logger systems (CR5000) and (CR-10X), both Campbell Scientific, Inc., from which hourly averages were calculated Vourlitis et al. (2011). The micrometeorological data set used in this work is the same used in the study prepared by Vourlitis et al. (2011), whose data are previously validated. Technical details such as precision, accuracy, and calibration can be found in Vourlitis et al. (2011); Moreira et al. (2017). All direct measurements used are listed in Table 1.

### 2.2.3 Measures of flux and concentration of CO$_2$

In Amazonia, the eddy covariance system has been widely used to measure the net CO$_2$ flux by the ecosystem. This system performs measurements by correlation of turbulent vortices from a sonic anemometer and an infrared gas chamber (Infrared

145 Gas Analyzer, IRGA), from which flux measurements of CO$_2$ (Carbon), water vapor (H$_2$O) and energy (sensible heat – H and latent heat – LE) are determined at high frequency, usually 10Hz. The data generated and recorded by the *eddy* system, deployed in flux towers, is normally adjusted by compilation software such as Alteddy 3.90 (Alterra, WUR, Netherlands), from which averages are taken every 10, 30 or 60 min Foken (2008). This system has been extensively described and improved in recent years Moncrieff et al. (1997); Aubinet et al. (2001); Aubinet (2012). The carbon flux data from these micrometeorological

150 towers are presented, using the classical sign convention in atmospheric science (negative flux indicates net ecosystem CO$_2$CO2 uptake).

## 2.3 Methods for calculating NEE and radiative effects of aerosols

### 2.3.1 Method to determine the net exchange of CO$_2$ in the ecosystem

The $NEE$ is obtained from turbulent flux measurements using the eddy covariance technique taking into account the storage

155 term S[CO$_2$] Aubinet (2012); Araújo et al. (2010). Micrometeorological sensors distributed vertically along the tower are essential for the $NEE$ calculations Hollinger and Richardson (2005), using continuous measurements of the CO$_2$ profile between soil and the top of the tower. Under these conditions, $NEE$ can be approximated by Equation 1:

$$NEE \approx FCO_2 + S[CO_2]_p \tag{1}$$

where $FCO_2$ is called "$CO_2$ turbulent flux", calculated by the *eddy* system, above the treetops Grace et al. (1996); Burba

160 (2013); $S[CO_2]_p$ is the vertical profile of the concentration of CO$_2$ or storage term (storage), considered a non-turbulent term, measured at discrete levels $z$, at thicknesses $\Delta z_i$, from near the ground surface to the point of measurement of covariance of turbulent vortices in the tower Finnigan (2006); Araújo et al. (2010); Montagnani et al. (2018). In this work, the vertical profile $S[CO_2]_p$ was stratified into 5 reference levels (1, 4, 12, 20, and 28 m)Vourlitis et al. (2011). Typical diurnal conditions consist of vector winds with speeds of 2.0 ms$^{-1}$ and u$^{\star}$ = 0.20 ms$^{-1}$ and predominant SSW and SE directions. Approximately 72% of

165 the accumulated flux originates within 1 km and the representativeness of the measured CO$_2$ flux (footprint) is approximately 520 m (upstream of the tower), following the model proposed by Schuepp et al. (1990). The concentrations [CO$_2$] were calculated following Aubinet et al. (2001) and Araújo et al. (2010), as reported by Vourlitis et al. (2011).

$$S[CO_2]_p = \frac{P_{air}}{RT_{air}} \int_0^z \frac{\partial [CO_2]}{\partial t} \, dz \tag{2}$$

Where: P$_{air}$ is the atmospheric pressure (Nm$^{-2}$), R is the molar constant of the gas (Nm mol$^{-1}$ K$^{-1}$) and T$_{air}$ the air

170 temperature in (°C).

### 2.3.2 Method to determine the solar irradiance of clear sky

The term clear sky was used here to designate the minimal influence of clouds and aerosols on the the solar radiation measured by the pyranometer. To estimate the amounts of direct solar radiation to the surface under minimally overcast sky conditions, the measurements $SW_{ia}$ of the AERONET 2.0 system (*cloudless*) observed under clear-sky conditions were used, that is, AOD $\leq 0.10$ Artaxo et al. (2022), in the absence of fire plumes. Under these conditions, we get the Equation 3; a polynomial fit of order 4, here, considered representative of the entire solar spectrum Meyers and Dale (1983). The model $S(t)_0$ obtained was used to derive the clear-sky instants at the surface (Fig. S4), between 07-17h (LT), according to the formulation below:

$$SW_{ia}\{AOD \leq 0.10\} \approx S(t)_0 = at^4 + bt^3 + ct^2 + dt + e \tag{3}$$

Where $S(t)_0$ is the clear-sky solar irradiance as a function of time, in $Wm^{-2}$. The parameters $(a,b,c,d,e)$ are the coefficients of the polynomial curve and $t$, the time, in local hours (LT). Figure 2 shows the mean diurnal cycle of the $SW_{ia}$ obtained from long-term aerosol measurements by the AERONET system under different pollution conditions. The plot illustrates the sensitivity of the method applied to determine the expected irradiance levels on the canopy forest $(S(t)_0)$ under varied atmospheric aerosol loads (AOD), C2, C4, and C6 curves. Markers C1, C3, and C5 represent averaged observations between 07:00-17:00 used to fit C2, C4, and C6 curves.

Using the long series of measurements of $AOD_a$ it was possible to obtain different curves $S(t)_0$ for each month of the year, taking into account the seasonal variations of the $SW_{ia}$ given in Equation 3. Figure S4 shows the seasonal variation of the $S(t)_0$ diurnal cycle throughout the year. The coefficients of the fit curves it listed in Table S1. To assess the consistency of the $S(t)_0$ model, obtained by $SWia$ AERONET data set, we compared the outputs calculated by Equation 3 with the clear-skies solar irradiance model available by the Meteoexploration (SolarCalculator).

### 2.3.3 Determination of relative irradiance

In practical terms, the relative irradiance $f$ expresses the relationship between incident solar radiation and that observed at the surface under a clear sky (AOD < 0.10) and "free" of clouds ($f > 1.0$). To determine it, it is necessary to calculate $S(t)_0$, given in the previous section. It is a parameter indicating the presence of clouds and/or pollution plumes with aerosols that scatter solar radiation, generally used in areas without direct instrumentation of cloud cover over the flux tower observation area. In these cases, $f$ is considered a key indicator in the detection of clouds and plumes of pollution from fires in the Amazon. For this, the observed amounts of $SW_{ia}$ on the forest canopy were normalized by the irradiance $S(t)_0$; both variables in $Wm^{-2}$, thus determining the quotient $f$ (dimensionless parameter), according to Equation 4 below.

$$f = \frac{SW_{ia}\{AOD_a > 0.10, cloudness\}}{S(t)_0\{AOD_a \leq 0.10, cloudless\}} \tag{4}$$

Where: $SW_{ia}$ is the total incident solar irradiance measured by the pyranometer ($Wm^{-2}$) under any atmosphere ($AOD_a$ > 0.10) and in the possibility of clouds (*cloudness*) and $S(t)_0$ is the clear sky solar irradiance ($Wm^{-2}$) on a flat surface
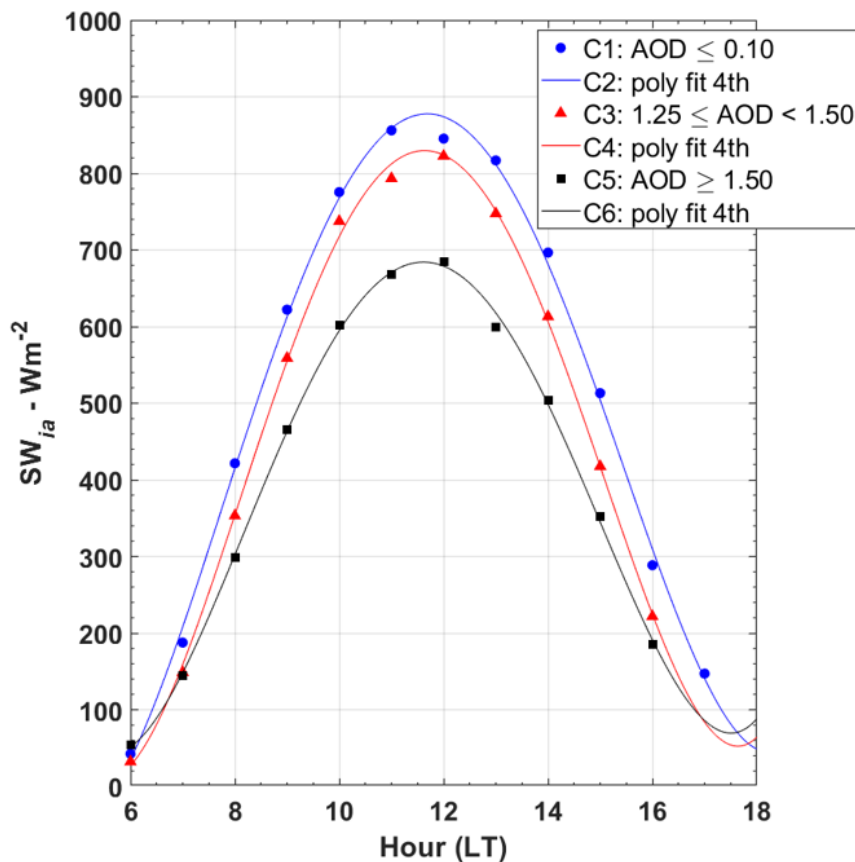
**Figure 2.** Incident solar irradiance under different sky conditions in Alta Floresta (1993 to 2018): clear-sky (C2 curve, AOD $\leq$ 0.10) and polluted-sky (C4 curves) and C6, AOD $\geq$ 1.25). The C1, C3, and C5 points curves

perpendicular to the sun's rays, without the attenuating effects of the atmosphere (clouds and burned) for a given time and place, ie $AOD_a \leq 0.10$ (*cloudless*). Values off close to zero represent cloudy and/or smoky-sky conditions, and values close to unity represent clear-sky conditions Gu et al. (1999); Oliveira et al. (2007); Jing et al. (2010); Cirino et al. (2014); Gao (2020).

205    Here, we used $f$ as a basis for comparison to detect the joint presence of clouds and aerosols from fires over the study area, since the experimental site does not have instrumentation for direct observation of cloud cover. Obtaining this parameter is extremely important because when using clear-sky solar radiation as a base, solar radiation measured under overcast skies becomes a new metric for observing cloudiness. This variable will be compared with the $NEE$ to assess the photosynthetic responses of the ecosystem to variations in the external environment.

9

### 2.3.4 Determining the clarity index

210 To determine the parameter $kt$ (here defined as brightness index) the extraterrestrial solar irradiance $S_{ext}$ was first calculated (depending only on orbital parameters). The index $kt$ is a coefficient of proportionality between the measurements of direct solar radiation to the surface and $S_{ext}$. This index expresses the direct solar radiation transmitted in the atmosphere Gu et al. (1999); Cirino et al. (2014). In a first approximation $kt$ indicates the transmissivity; the degree of transparency of the atmosphere to solar radiation at a given time and place, while $f$ is a parameter of comparison more sensitive to the presence of

215 radiation-scattering aerosols and clouds. Here, $kt$ and $SZA$ were used as predictors of the diffuse component of Gu et al. (1999); Cirino et al. (2014) radiation. For the calculation of the irradiance $S_{ext}$ some parameters and variables are also needed such as the solar constant of the Earth ($S_{ext}^t$), the latitude of the location ($\varphi$), solar declination ($\delta$), hour angle ($h$) and mean square distance between the Earth and the Sun Gates (1980). The determination of $S_{ext}$ takes into account the angle of incidence of the solar rays and, therefore, the variations in the amounts of solar radiation at the surface, modulated by the $SZA$.

220 Under these conditions, $kt$ can be expressed according to Equation 5:

$$kt = \frac{\text{SW}_i \{AOD > 0.10, cloudiness\}}{S_{ext}} \tag{5}$$

Where $\text{SW}_i$ is the short wave radiation measured by the pyranometer (Wm$^{-2}$) (Table 1) and $S_{ext}$ the extraterrestrial solar irradiance (Wm$^{-2}$) estimated on a perpendicular surface to the sun's rays, without the attenuating effects of the atmosphere for a given time and place, expressed according to 6.

225 $$S_{ext} = S_{ext}^t \left(\frac{\bar{D}}{D}\right)^2 \times cos(z) \tag{6}$$

In this equation $S_{ext}^t$ is the Earth's solar constant ($\approx 1367$ Wm$^{-2}$), $\bar{D}$ is the average Earth-Sun distance ($\sim 1.49$ x $10^6$ km), D is the Earth-Sun distance on a given Julian day, and cos (z) the cosine of the solar zenith angle (SZA), calculated as proposed by Bai et al. (2012). This calculated index was used to establish the diffuse solar radiation, as described in detail in the next section.

### 230 2.3.5 Determination of diffuse PAR radiation

To determine the diffuse component of the total PAR ($PAR_d$), we adopted the procedures of Spitters et al. (1986) and Reindl et al. (1990), widely used in the literature when there are no direct measurements of radiation $PAR_d$ Gu et al. (1999); Jing et al. (2010); Zhang et al. (2010); Bai et al. (2012). The detailed calculation can be found in the one performed by Gu et al. (1999). The estimate is performed by deriving the diffuse PAR radiation according to the formulation below (Spitters, 1986).

235 $$PAR_d = \left[\frac{1 + 0.3\left(1 - q^2\right)q}{1 + \left(1 - q^2\right)\cos^2\left(90 - z\right)\cos^3\left(z\right)}\right] \times \text{PAR}_i \tag{7}$$

Where $PAR_d$ is the incidence of the diffuse (total) PAR radiation flux ($\mu$mol photon m$^{-2}$s$^{-1}$), in the near-infrared range, in a horizontal plane to the Earth's surface, while $q$ is a coefficient of proportionality used to denote the ratio of the total diffuse radiation to a given amount of irradiance (SW$_i$) at the surface, under a given condition of the sky (Wm$^{-2}$). The parameter $q$ is expressed considering ranges of variation for the index $kt$ Gu et al. (1999). To express the diffuse fraction of PAR radiation

240 ($PAR(D)_F$) we use the relationship between $PAR_d$ and PAR$_i$ Spitters et al. (1986). In the absence of direct measurements of diffuse solar radiation, the procedures reported by these authors are still widely used Jing et al. (2010); Cirino et al. (2014); Moreira et al. (2017).

### 2.3.6 Determining the efficiency of light use

Another important parameter in this kind of study is the light use efficiency ($LUE$), which expresses the efficiency of light

245 use in photosynthetic processes by the canopy. It is defined as the ratio between $NEE$ and PAR$_i$. Several other procedures have been used to approximate the $LUE$, some use the coefficient of proportionality between the $NEE$ and the $PAR_d$ Moreira et al. (2017) radiation, and others use temperature measurement directly on the leaf of the trees (LI-COR) to capture the photosynthetic response as a function of the variation in light intensity Doughty et al. (2010). Canopy radiative transfer codes with validated physical parameterizations for different leaf types are also used Mercado et al. (2009). Here, for practical

250 reasons, we used the procedures applied by Jing et al. (2010) and Cirino et al. (2014), according to Equation 8, where $LUE$ is given in percentage values.

$$LUE \approx \left( \frac{NEE}{\text{PAR}_i} \right) \tag{8}$$

### 2.3.7 Determining leaf canopy temperature

We used the parameterization proposed by Tribuzy (2005) to estimate $CL_T$ (leaf canopy temperature), obtained from field

255 experiments carried out in central Amazonia, located approximately 60-70 km NW from the center of Manaus-AM, with micrometeorological measurements and temperature measured with thermocouples on leaves during the dry season (July-August/2003) and rainy seasons (December 2003 to February 2004), respectively. Doughthy et al. (2010) used alternative procedures based on pyrometer measurements to estimate leaf canopy temperature in the Tapajós National Forest (FLONA-Tapajós), in Santarém-PA, obtaining similar $CL_T$ diurnal cycles. Here, in the absence of direct leaf temperature measurements

260 or data from pyrgeometers operated above the canopy to measure the emission of long-wave radiation from the LW$_c$ surface in the experimental tower (Table 1), we estimate the leaf canopy temperature ($CL_T$) through the formulation proposed by Tribuzy (2005). The final equation obtained is expressed as a function of relative air humidity (RH$_{air}$) and PAR$_i$ radiation, as shown below:

$$CL_T = [(2.48 \cdot 10^{-6}(\text{RH}_{air})^2 - 1.82 \cdot 10^{-4}(\text{RH}_{air}) - 1.83 \cdot 10^{-6}(\text{PAR}_t) + 0.0363)]^{-1} \tag{9}$$
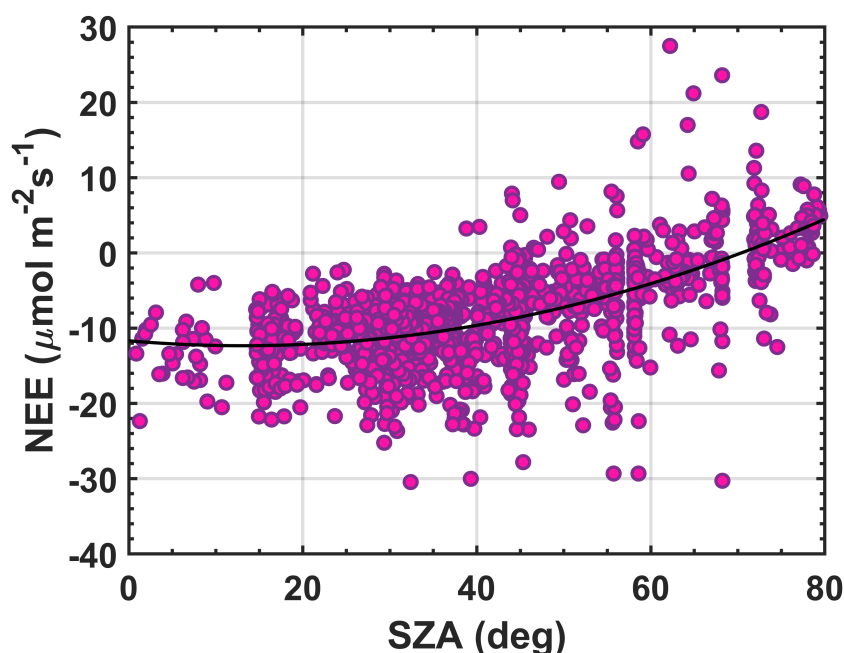
**Figure 3.** Correlation between $NEE$ and $SZA$ for clear sky conditions ($f \approx 1.0$), in the Cláudia Municipality. The black curve indicates the 2nd order polynomial fit obtained ($NEE(sza)_0$).

### 2.3.8 Determination of clear sky NEE

The $NEE$ observed on clear days (AOD $< 0.1$ and clear) was also used as a basis for comparison days with high aerosol loading. The Fig. 3 illustrates the behavior of the $NEE$ under clear sky conditions ($f \approx 1.0$). The polynomial fit obtained is used to determine the clear sky $NEE(sza)_0$ as a function of $SZA$ variations, between Jun2005-Jul2008. The correlation curve found is consistent with the behavior observed in previous studies Gu et al. (1999); Cirino et al. (2014). The equation below was used to estimate the expected $NEE$ under the above-mentioned conditions.

$$NEE(sza)_0 = p_1 SZA^2 + p_2 SZA + p_3 \tag{10}$$

Where $NEE(sza)_0$ is the $NEE$ typically found on clear sky days ($\mu$mol m$^{-2}$s$^{-1}$). The parameters $p_1$, $p_2$ and $p_3$ the coefficients of the polynomial curve obtained, respectively equal to: $0.0038$, $-0.99$ and $-12$. Like $f$, $\%NEE$ was used here as a basis for comparison for the maximum negative values observed between Jun2005-Jul2008, assuming, in this analysis, the absence of water stress and nutrient deficiency in the studied period Gu et al. (1999); Oliveira et al. (2007); Doughty et al. (2010); Cirino et al. (2014).

Changes in observed $NEE$ versus $NEE$ under clear sky conditions were used to determine the percentage effect of aerosols on $NEE$. The $\%NEE$ was calculated by the following relationship Bai et al. (2012); Gu et al. (1999); Oliveira et al. (2007):

$$\%NEE = \left( \frac{NEE(sza) - NEE(sza)_0}{NEE(sza)_0} \right) \times 100 \tag{11}$$

To largely eliminate solar elevation angle interference in the analysis of changes in $\%NEE$ versus $f$, we grouped the data into $SZA$ ranges of 20-25°. This interval was small enough to minimize the effects of solar uplift during the day and to represent changes in $NEE$ as a function of $f$ in response to changes in $NEE$ flux due to aerosols and/or clouds alone. This interval also ensured sufficient sample size for statistical analyses. $SZA$ intervals smaller than 15° significantly reduced the sample size, making it impossible to develop a robust statistical analysis Gu et al. (1999). Values above 50 or around 0 (solar angles very close to the horizontal and vertical plane, respectively) were, in general, very contaminated by clouds Gu et al. (1999); Cirino et al. (2014).

### 2.4   Data analysis procedures

Computational routines were developed for compilation, certification, organization, and analysis of the variables presented in Table 1. We performed fitting curves and mathematical or statistical calculations with the packages available in MATLAB (2013). For data quality control, non-physical values outside acceptable levels were excluded from the database, totaling a loss of 3% of the total set of valid measurements (approximately 3,600 sampled points). Data analysis consists of three fundamental steps: (1) variation of solar radiation with optical depth $AOD_a$ analyzed as a function of irradiance $f$; (2) effects of aerosols and clouds on the net exchange of $CO_2$ at the forest-atmosphere interface and, finally, (3) quantification of photosynthetic performance as a function of pollution loads, from which to extract if the biological critical or optimal values for environmental (exogenous) factors such as $d$, $T_{air}$, $CL_T$ and VPD (Vapour-Pressure Deficit). Photosynthetic performance, in all cases, is analyzed as a function of $NEE$. In the end, the net percentage variation of the photosynthetic activity of the forest ($\%NEE$) is evaluated as a function of the irradiance $f$. Non-linear regression was used to determine functional relationships between NEE and other radiation variables. The relationships found are evaluated from the Poisson correlation and tabulated in terms of basic descriptive statistical parameters such as coefficient of determination ($R^2$) and significance level ($P_{value}$) with margin confidence of 95%. Basic descriptive statistics are also applied to the data to obtain mean values, medians, percentiles, and standard deviations for the measured and estimated variables. Table 2 lists indirect variables, calculated from the dataset listed in Table 1.

## 3   Results and Discussions

### 3.1   Average daily cycle of net exchange of $CO_2$

The average daily pattern of $NEE$ observed in 2005-2008 follows the typical pattern of tropical forests in the Amazon and other tropical forests Gu et al. (1999); Niyogi et al. (2004); von Randow et al. (2004); Araújo et al. (2010); Doughty et al. (2010). The maximum negative fluxes average $-13.7 \pm 6.2$ $\mu$mol m$^{-2}$s$^{-1}$, often observed around 10-11h (LT), and the maximum positive $+6.8 \pm 5.8$ $\mu$mol m$^{-2}$s$^{-1}$, approximately constant during the night period between 19h and 05h (LT),

**Table 2.** List of indirect (calculated) variables, symbols, and measurement units of derived quantities, according to the cited body of literature.

| Indirect Measures | Symbols | Units | Literature |
|---|---|---|---|
| $CO_2$ Net Exchange | $NEE$ | $\mu$mol m$^{-2}$s$^{-1}$ | Vourlitis et al. (2011) |
| Vapour Pressure Deficit | $VPD$ | hPa | Vourlitis et al. (2011) |
| Clear Sky Solar Irradiance | $S(t)_0$ | Wm$^{-2}$ | (Author) |
| Solar Zenith Angle | $SZA$ | Degrees | Bai et al. (2012) |
| Relative Irradiance | $f$ | - | Cirino et al. (2014) |
| Clarity Index | $kt$ | - | Gu et al. (1999) |
| Extraterrestrial Solar Irradiance | $S_{ext}$ | Wm$^{-2}$ | Gu et al. (1999) |
| Diffuse PAR Radiation | $PAR_d$ | $\mu$mol phot. m$^{-2}$s$^{-1}$ | Gu et al. (1999) |
| Diffuse PAR Fraction | $PAR(D)_F$ | - | Gu et al. (1999) |
| Efficiency of Light Use | $LUE$ | - | Jing et al. (2010) |
| Leaf Canopy Temperature | $LC_T$ | °C | Tribuzy (2005) |
| Clear Sky NEE Exchange | $NEE(sza)_0$ | $\mu$mol m$^{-2}$s$^{-1}$ | Cirino et al. (2014) |
| Relative NEE Exchange | $\%NEE$ | % | Cirino et al. (2014) |

considering the data for the entire year. We observed a slight difference in the pattern of the daily cycle of the $NEE$ between
310   the wet and dry seasons (Fig. (4)), with $CO_2$ absorption peaks about 10-15% lower (i.e, less negative) during both seasons ($<$ 0.6 $\mu$mol m$^{-2}$s$^{-1}$), when compared to Vourlitis et al. (2011). Our results also show a shift (an advance) in the peak absorption of $CO_2$ from the wet-to-dry season, from about 12h (LT) to 10h (LT), respectively (Fig. 4).

Seasonal variations in water availability, nutrients, radiation, temperature, VPD, and pollution are counterbalanced throughout the year, producing an average seasonal behavior without significant differences in $NEE$. Vourlitis et al. (2011) showed
315   similar monthly variations with more negative magnitudes during the day in the rainy months ($-9.0$ $\mu$mol m$^{-2}$s$^{-1}$, between November-February) and less negative during the light hours in the dry months ($-7.7$ $\mu$mol m$^{-2}$s$^{-1}$, between May-August). During nighttime these values are respectively equal to $+5.4$ $\mu$mol m$^{-2}$s$^{-1}$ and $+7.4$ $\mu$mol m$^{-2}$s$^{-1}$. The general balance between these fluxes reveals 'carbon uptake' of $-0.12$ $\mu$mol m$^{-2}$s$^{-1}$ and $-0.18$ $\mu$mol m$^{-2}$s$^{-1}$ during the wet and dry seasons, respectively. The maximum rates of photosynthesis and leaf canopy respiration were observed in October-November, which
320   are the first months of the rainy season Vourlitis et al. (2011).
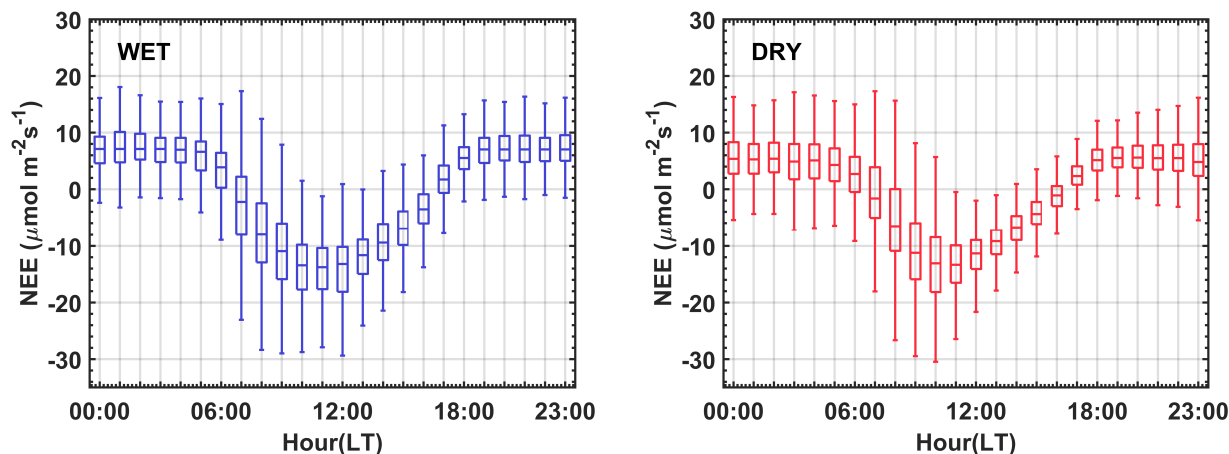
**Figure 4.** $NEE$ average hourly cycle between June/2005 and July/2008, during the rainy (WET) and less rainy (DRY) seasons in a semide-ciduous forest in the Cláudia municipality, 50 km northeast of Sinop, Mato Grosso. The standard deviation is shown as vertical bars.

## 3.2 The influence of aerosols on solar radiation

The impact of aerosol particles by fires on the $SW_i$ flux is evaluated as a function of $f$, $AOD_a$, $SZA$, $PAR(D)_F$ and $PAR_i$. Fig. 5 (top panel) shows the behavior of the relative irradiance $f$ for different levels of $AOD_a$ pollution, in the $SZA$ ranges between 20-50°. A close and statistically significant relationship between $f$ and $AOD_a$ is observed with p-value $< 0.01$ and 325 $R^2$ of about 0.92 (Table 3). An approximately linear relationship is observed in which $f$ decreases by about 40-60% when the $AOD_a$ varies from 0.10 to 5.0. No statistically significant difference was observed between mornings and afternoons. There is only a slight increase of $\approx$ 5-20% (on average) in the value of $f$ between late mornings and afternoons, attributed here to the multiple scattering of solar radiation due to the formation of clouds near the tower Gu et al. (2001). For $SZA$ angles between 20 and 50°, there is a strong reduction in the amounts of $SW_i$ ($225 \pm 50$ Wm$^{-2}$) associated mainly with the increase in the 330 concentration of aerosols emitted by local fires or transported regionally during the burning season. Oliveira et al. (2007) and Cirino et al. (2014) reported results about 2-3 times lower for 20-30% reductions in $f$ and AOD increase from 0.1 to 0.8, in FLONA-Tapajós (Santarém-PA) and central Amazon (K4), in Manaus-AM.

Figure 5 (bottom panel) shows the fraction of diffuse radiation calculated as a function of $AOD_a$, with a close statistical relationship observed ($R^2 = 0.98$ and 0.96) for the morning and afternoon hours (Table 3). Due to the reduction in the instan-335 taneous fluxes of $SW_i$ an increase of about up to 85% in diffuse radiation is observed when the $AOD_a$ increases from 0.10 to 5.0. These results are consistent with previous studies carried out in the Brazilian Amazon Doughty et al. (2010); Cirino et al. (2014); Rap (2015); Moreira et al. (2017); Malavelle et al. (2019); Bian et al. (2021) and around the world Niyogi et al. (2004); Jing et al. (2010); Rap (2015); Rap et al. (2018) and proves to be particularly important due to to the ability of $PAR_d$ to penetrate more efficiently into the leaf canopy, and under certain conditions, increase ecosystem in carbon uptake.
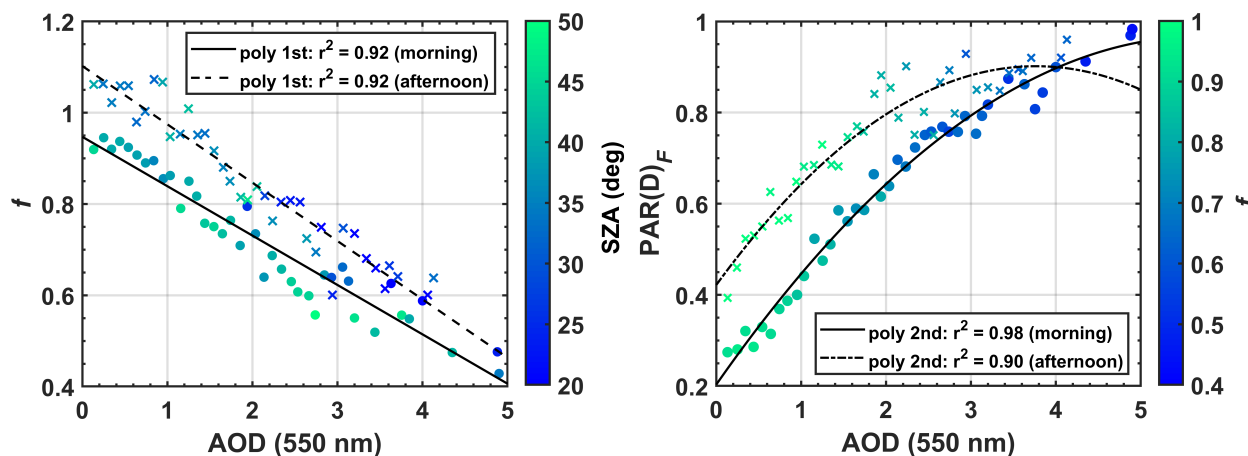
**Figure 5.** 3D-correlation between $f$ and $PAR(D)_F$ with increasing $AOD_a$ for different values $SZA$ (top panel) and irradiance $f$ (bottom panel) in semi-deciduous forest in the Cláudia municipality, 50 km northeast of Sinop-MT (2005-2008).
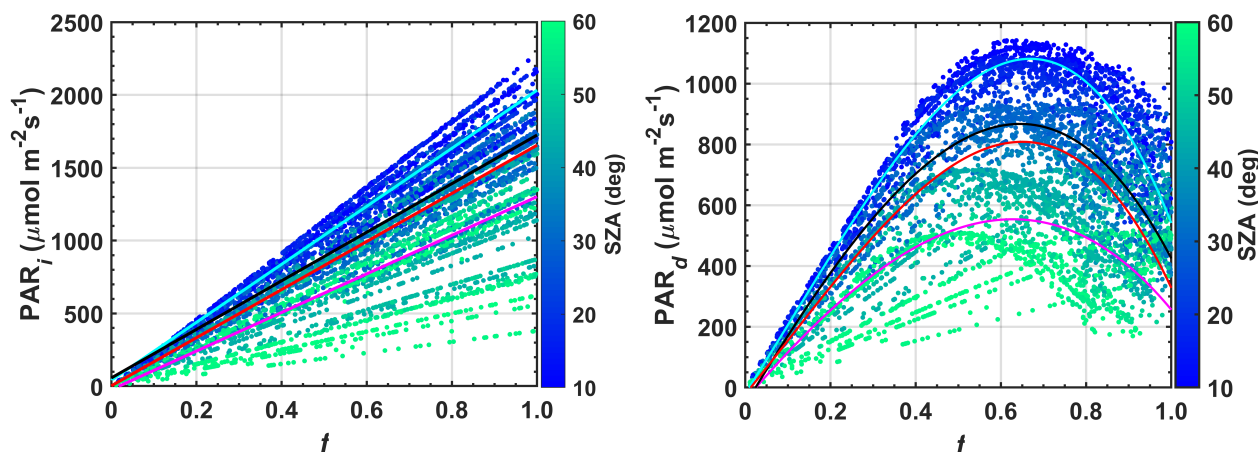
**Table 3.** Polynomial adjustments (Fig. 5), coefficients and statistics for the morning and afternoon periods in the micrometeorological tower in Cláudia-MT (2005-2008). $R^2$ is the correlation coefficient, $\Delta \mathbf{SW}_i$ is the incident shortwave radiation amount, and STD is the Standard Deviation.

| Settings | | Period | Coefficients | | | Statistics | |
|---|---|---|---|---|---|---|---|
| Polynomial Functions | | Local Hours | $a$ | $b$ | $c$ | $R^2$ | $\Delta \mathbf{SW}_i$ (STD) |
| $f$ | poly fit 1st | 07-12h | $-0.11$ | 0.95 | | 0.92 | -200 ($\pm$ 50) |
| | | 12-17h | $-0.13$ | 1.10 | | 0.92 | -250 ($\pm$ 80) |
| $PAR(D)_F$ | poly fit 2nd | 07-12h | $-0.023$ | 0.27 | 0.20 | 0.98 | -97 ($\pm$ 30) |
| | | 12-17h | $-0.034$ | 0.25 | 0.42 | 0.90 | -118 ($\pm$ 42) |

## 3.3 The influence of aerosols on PAR radiation

Figure 6 shows the behavior of the radiation $PAR_i$ and $PAR_d$ as a function of $f$ and $SZA$. For reductions in $f$ of $\approx 40\%$ ($f$ ranging from 1.0 to 0.6) there were strong reductions in $PAR_i$ ($\sim 750 \ \mu$ mol m$^{-2}$s$^{-1}$) and a corresponding 55% increase in diffuse radiation $PAR_d$ ($\sim 600 \ \mu$mol m$^{-2}$s$^{-1}$) between July-November. These numbers indicate a strong reduction in $PAR_i$ as pollution levels increase and change from clear sky conditions (AOD $\leq 0.10$, $f \sim 1.0$) to aerosol smoky sky conditions of fires (AOD $\gg 0.1$, $f \ll 1.0$).

$PAR_i$ decreased almost linearly wich increasing $f$ (Fig. 6, top panel). The relationship between $PAR_d$ radiation and $f$ does not show a linear behavior (Fig. 6, bottom panel). $PAR_d$ values reach maximum values (779-1080 $\mu$mol m$^{-2}$s$^{-1}$) for values of $f$ between 0.63 and 0.66 (reductions of 37 %-34%) for ranges $SZA$ (20-40°). As will be seen below, these values

**Figure 6.** 3D-correlation between $f$, $PAR_i$ (top panel) and $PAR_d$ (bottom panel) for different $SZA$ values. The blue, black, magenta and red lines are the polynomial curves adjusted to the analyzed $SZA$ variation ranges, respectively equal to 0-20º, 20-40°, 40-60°, and 0-60°, in semi-deciduous forest in the Cláudia municipality, 50 km northeast of Sinop-MT (2005-2008).

**Table 4.** Polynomial adjustments (Fig. 6), coefficients, and statistics for the morning and afternoon periods in the micrometeorological tower in Cláudia-MT (2005-2008). $\mathbf{C}p\,(x_v, y_v)$ is the critical point of the fit curve, where the derivative is equal to zero.

| Settings | Angles | Coefficients | | | | Etatistic | |
|---|---|---|---|---|---|---|---|
| **Polynomial Functions** | **SZA** | *a* | *b* | *c* | *d* | **R**$^2$ | $\mathbf{C}p\,(x_v, y_v)$ |
| $PAR_i$ poly 1st | 0-20° | $+1.5 \times 10^3$ | $+56$ | | | 0.92 | |
| | 20-40° | $+2.0 \times 10^3$ | $+41$ | | | 0.86 | |
| | 40-60° | $+1.7 \times 10^3$ | $+57$ | | | 0.64 | |
| | 0-60° | $+1.3 \times 10^3$ | $-23$ | | | 0.67 | |
| $PAR_d$ poly 3rd | 0-20° | $-2.5 \times 10^3$ | $+8.4 \times 10^2$ | $+2.2 \times 10^3$ | $-19$ | 0.92 | (0.66, 1080) |
| | 20-40° | $-1.3 \times 10^3$ | $-5.6 \times 10^2$ | $+2.3 \times 10^3$ | $-56$ | 0.66 | (0.63, 846) |
| | 40-60° | $-6.4 \times 10^2$ | $-7.0 \times 10^2$ | $+1.6 \times 10^3$ | $-41$ | 0.42 | (0.61, 529) |
| | 0-60° | $-2.0 \times 10^3$ | $+5.8 \times 10^2$ | $+1.7 \times 10^3$ | $-22$ | 0.40 | (0.63, 779) |

are considered critical for maximum $CO_2$ absorption rates (maximum-negative $NEE$). The 50% increase in $PAR_d$ can be
350  explained by aerosol dispersion during the biomass burning season (July-November), with results mainly attributed to the dense
layer of radiation-scattering aerosols, typical of Biomass Burning Organic Aerosols (BBOA) aerosols Shilling et al. (2018);
de Sá et al. (2019). The polynomial fits, coefficients, and inflection points are displayed in Table 4.

17

### 3.4 The indirect effect of aerosols on the use of light efficiency by the forest

Due to the burning season, there was a well-defined monthly variation of $AOD_a$, as shown in the previous sections. Since fires
355 are the main cause of changes in the physical and chemical composition of the atmosphere throughout the year Martin et al.
(2010b, a); Artaxo et al. (2013, 2022), statistically significant reductions were found for the SW$i$ flux and radiation PAR$_i$.
This section mainly evaluates the optimal levels of PAR$_i$ radiation, as well as the effects of changes in the efficiency of solar
radiation use by the forest ($LUE$). The $LUE$, here, is expressed in terms of the quotient between the fluxes $NEE$ and PAR$_i$,
Equation 8, as already mentioned in the section before (2.3.6). The analyses are performed as a function of PAR$_d$ radiation,
360 from which the maximum efficiency of light use for the studied semideciduous forest is determined.

Under smoky sky conditions ($AOD \gg 0.10$), carbon assimilation gradually increases with increasing total PAR radiation
(PAR$_i$) reaching maximum saturation around 1550 and 1870 $\mu$mol m$^{-2}$s$^{-1}$ in the range between 20-50° $SZA$, values for
which the maximum $NEE$ (negative) occurs around $-23$ $\mu$ mol m$^{-2}$s$^{-1}$. Under clear sky conditions, considering the same
$SZA$ range, the maximum saturation (maximum negative $NEE$), occurs around 2100-2300 $\mu$mol m$^{-2}$s$^{-1}$, that is, around
365 $-18$ $\mu$mol m$^{-2}$s$^{-1}$ (Fig. 7, top panel). To complement this analysis, the $NEE$ flux was normalized by the radiation PAR$_i$ and
plotted against the $PAR(D)_F$ during days with high aerosol loading in the burning season (Fig. 7, bottom panel). Under these
conditions, it is observed that the forest reaches maximum $NEE$ fluxes on smoky days and not under clear sky conditions.
The results reveal that smaller amounts of energy are needed for the forest to reach maximum saturation on non-polluted
days. The analyses presented in Fig. 7 confirm greater photosynthetic efficiency under smoky sky conditions for the studied
370 semideciduous forest ecosystem, results compatible with field observations Oliveira et al. (2007); Doughty et al. (2010); Cirino
et al. (2014) and by numerical modeling in the Amazon Rap (2015); Moreira et al. (2017); Malavelle et al. (2019); Bian et al.
(2021) and the world Rap et al. (2018). Due to the physicochemical nature of the BBOA and its intrinsic properties Cirino et al.
(2018); Adachi et al. (2020) the radiation $PAR_d$ affects the $NEE$ and the functioning of several Amazon forest ecosystems
Rap (2015); Rap et al. (2018); Bian et al. (2021), especially where tree species adapted to low light conditions occur, for
375 example, in the leaf sub-canopy of Amazonian forests Mercado et al. (2009).

Photosynthetic efficiency ($LUE$), closely linked to the canopy's ability to convert solar energy into biomass, is $\sim$ 1-2% for
the studied forest, indicating loss or rejection of a large part of the solar energy available for photosynthesis. However, for high
values of $PAR_d$, close to 1.0, peaks of up to 3% in photosynthetic efficiency are observed. In situations where the diffuse
fraction total maximum values, the values of $AOD_a$ are on average greater than 1.0 and $f \ll 1.0$. These findings corroborate
380 the previous analyses and reinforce the presence of radiation-scattering aerosols emitted by the fires over the studied area.
Although there is great uncertainty (high standard deviation) in the behavior of $LUE$ with increasing radiation $PAR_d$, there is
a gradual, approximately linear increase in the values of $LUE$ in the range of radiation $PAR_d$ between 0.20-1.0. This behavior
is peculiar to tall vegetation with a generally leafy canopy of tropical forests, which are more sensitive to the transfer of $PAR_d$
radiation from the top canopy to the bole. In short-stature vegetation, as in the semiarid region of northeast China (e.g., grasses),
385 the $LUE$ remains approximately constant even for high values of $PAR_d$ generated by aerosols and clouds Jing et al. (2010).
Overall, however, the $LUE$ is low for many vegetation types, typically between 1-3%.
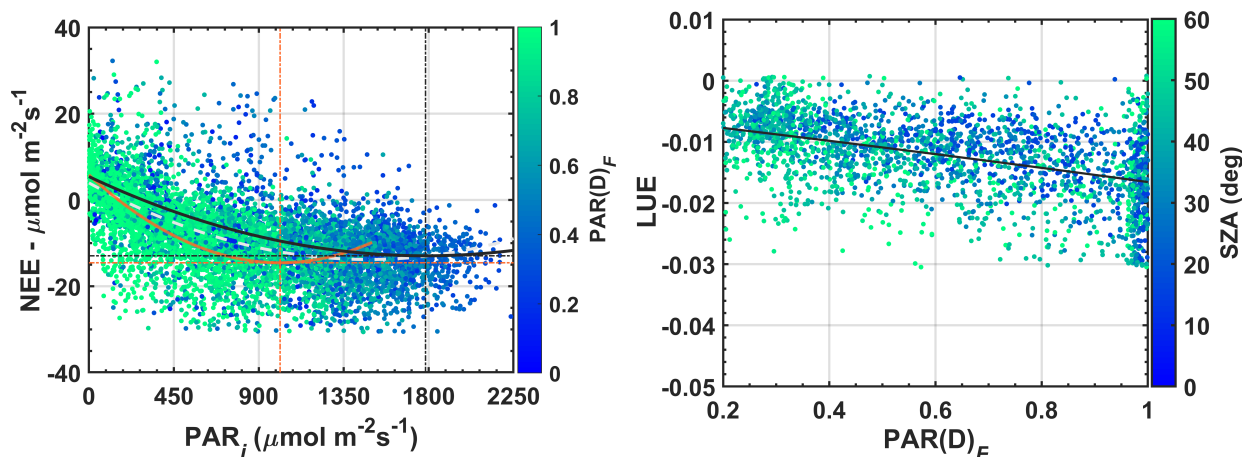
**Figure 7.** $NEE$ as a function of radiation, $PAR_i$ for measurements between 08h and 17h LT (top panel). The bottom panel shows the $LUE$ as a function of the fraction $PAR(D)_F$ ($R^2 = 0.21$, the value of $p < 0.001$) for an area of semideciduous forest located in the municipality of Cláudia- MT, 50 km north of Sinop, between Jun2005-Jul2008. The orange and black lines denote, respectively, observations $PAR(D)_F \geq$ 0.60 and observations $f \approx 1.0$ (clear-sky conditions). The orange and black vertical lines indicate the global minima of the polynomial curves.

### 3.5 The net absorption of CO$_2$ due to aerosols from fires

The Equation 11 and Equation 4 allowed us to evaluate the behavior of the ratio between the $\%NEE$ and the irradiance $f$ for intervals $SZA$ from 0-75°. This procedure was adopted to minimize the effects of solar elevation and air temperature on
390 the $NEE$ flux throughout the day Gu et al. (1999); Cirino et al. (2014). The intervals every 25° ensured the smallest possible $SZA$ variations and the largest possible number of points within the sample space necessary for statistical analyses. For each $SZA$ interval analyzed, the average $\%NEE$ was evaluated in *bins* of $f$ equal to 0.1, calculated separately (Fig. 8). The critical points and the coefficients of curves for all data (between 0-75° SZA) are shown in the supplementary material (Fig. S6, Table S2). On average, an average (absolute) increase of approximately 7.0 $\mu$mol m$^{-2}$s$^{-1}$ in carbon uptake was observed relative
395 to clear sky conditions ($NEE(sza)_0$), when $f$ varied from 1.1-1.0 to 0.66, results for the $SZA$ range between 0-75° (Fig. 8, top panel). The 7.0 $\mu$mol m$^{-2}$s$^{-1}$ increase represents a 20-70% increase in $NEE$ flux. This increase, strongly linked to the increase in aerosol concentration by fires, is mainly explained by the 50% increase in radiation $PAR(D)_F$ (approximately 450 $\mu$mol m$^{-2}$s$^{-1}$ in the stream $PAR_d$) and 35-40% reduction in the irradiance $f$ when the AOD$_a$ varies from 0.10 to 5.0 (Fig. 5, bottom panel).

400 Oliveira et al. (2007) and Cirino et al. (2014)(2014) showed a relative increase of about 30% for $f$ values ranging from 1.1 to 0.80. The negative variations in $f$, also indicated a high pollution load for fires at the site (AOD between 0.10-2.5) (Fig. 5, bottom panel) producing statistically significant reductions of up to 35% in the PAR radiation flux and a 47% increase in $PAR(D)_F$ (Fig. 5, Fig. 6, both bottom panel). These studies showed that the increase in carbon uptake, in the presence of
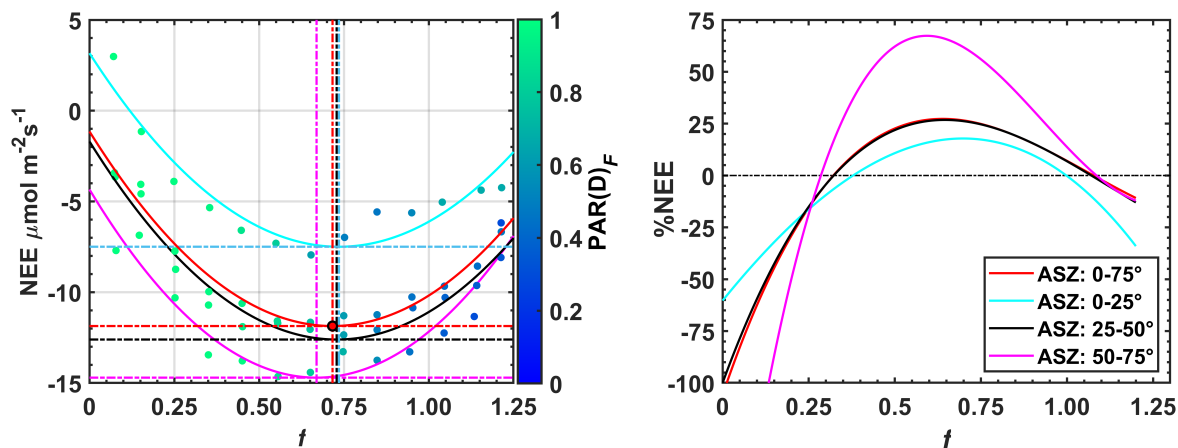
**Figure 8.** Variability of $NEE$ with $f$ for various $SZA$ ranges in the top panel. The $\%NEE$ as a function of the irradiance $f$ for the same $SZA$ intervals is shown in the bottom panel. These graphs include the effects of aerosols in the experimental area of Cláudia-MT, between 2005-2008.

aerosols and clouds, becomes smaller and similar in both locations for $SZA$ bands $< 20$. Solar radiation suffers less scattering

405   near the zenith ($SZA \sim 10°$) due to particles suspended in the atmosphere due to the narrowing of the optical path, reducing the effects of diffuse radiation on the photosynthetic process. These results, in particular, are generally repeated for the studied semi-deciduous forest of Mato Grosso, but a strong increase of 70% in $\%NEE$ is observed for lower $SZA$ ranges (between 50-75%), in the early hours of the day, between 8-10h (LT), while in the Jaru Biological Reserve (JBR) the biggest increases are concentrated in the $SZA$ ranges between 10-35°, close to midday, or in the morning-afternoon Oliveira et al. (2007). At

410   K34, in Manaus, the maximum absorptions and the maximum $\%NEE$ occur do not exceed 20% and the effects of aerosols and clouds operate together. The individual radiative influences of clouds and aerosols are difficult to quantify because satellite AOD observations have a low temporal resolution. Similar results were observed by Doughty et al. (2010) in FLONA-Tapajós, central Amazon. In general, higher standard deviations are found in regions most heavily impacted by aerosols, such as Ji-Paraná (RO) and Altafloresta (MT). Because aerosol concentrations are relatively lower in FLONA-Tapajós (PA) and Manaus

415   (AM), the standard deviations are lower. Table 5 lists the coefficients of the adjustments found between $\%NEE$ and $f$ for each of the considered ranges $SZA$, as well as the critical points (herein called biological optimum) for the irradiance values $f$ and $NEE$ flux ($\mu$mol m$^{-2}$s$^{-1}$).

These results are important as a large part of the Amazon area is frequently impacted by the presence of aerosols in small amounts (low AOD), similar to those observed in the north of the Amazon basin, in Manaus-AM. In regions with high rate

420   of deforestation and biomass burning, however, increases in $CO_2$ absorption are significant and can have major impacts on the carbon budget of the Amazon forest. Over dense forest ecosystems of central Amazon, $CO_2$ absorption peaks are often observed at higher and narrower intervals of f, generally between 1.1 to 0.80; especially for dense forest ecosystems Gu et al. (1999); Yamasoe et al. (2006); Oliveira et al. (2007); Doughty et al. (2010), which is different from grasslands and temperate

**Table 5.** Polynomial adjustments (Fig. 8), coefficients, and statistics for the periods between 07-17h (LT) in the micrometeorological tower 50 km from Sinop-MT, in the municipality of Cláudia, between 2005-2008.

| Settings | Angles | Coefficients | | | | Statistic | |
|---|---|---|---|---|---|---|---|
| **Poly fit 2nd** | **ASZ** | *a* | *b* | *c* | *d* | $\mathbf{R}^2$ | $\mathbf{C}p\,(x_v, y_v)$ |
| | 0-25° | +23 | −31 | −4.3 | | 0.88 | (0.74, -07.50) |
| | 25-50° | +21 | −30 | −1.7 | | 0.95 | (0.73, -12.61) |
| NEE | 50-75° | +20 | −29 | +3.1 | | 0.88 | (0.67, -14.71) |
| | 0-75° | +21 | −30 | −1.1 | | 0.97 | (0.72, -11.90) |
| **Poly fit 3rd** | **ASZ** | *a* | *b* | *c* | *d* | $\mathbf{R}^2$ | $\mathbf{C}p\,(x_v, y_v)$ |
| | 0-25° | −38 | $−1.1 \times 10^2$ | $+2.1 \times 10^2$ | −60 | 0.88 | (0.70, 20.06) |
| | 25-50° | $+1.5 \times 10^2$ | $−4.9 \times 10^2$ | $+4.5 \times 10^2$ | $−1.0 \times 10^2$ | 0.97 | (0.68, 26.68) |
| %NEE | 50-75° | $+5.4 \times 10^2$ | $−1.5 \times 10^3$ | $+1.2 \times 10^3$ | $−2.4 \times 10^2$ | 0.97 | (0.58, 56.77) |
| | 0-75° | $+1.7 \times 10^2$ | $−5.4 \times 10^2$ | $+4.9 \times 10^2$ | $−1.1 \times 10^2$ | 0.98 | (0.66, 27.05) |

forest, where the maximum net CO2 uptake is generally found in the range $f$ between 1.0-0.5 Gu et al. (1999); Niyogi et al.
425 (2004); Jing et al. (2010); Zhang et al. (2010).

The mechanisms to explain the variation in $\%NEE$ with the irradiance $f$ are complex and influenced by the dynamics of the Planetary Boundary Layer (PBL) throughout the day, including transport of regionally transported and locally emitted burning emissions. For the semideciduous forests studied here, an accumulation of aerosols from fires during the night hours (19h to 06h, LT) may be associated with greater stability in the PBL during the fire season (lower values in wind speed, reduction in
430 convection and boundary layer narrowing). These factors can increase the concentration of aerosols ($AOD_a$) during the night, with important effects on the $CO_2$ absorption capacity ($\%NEE$) observed in the early daytime hours ($SZA$ values between 50-75°.

Future studies may elucidate the dynamic effects of PBL on the photosynthetic capacity of forests in the Amazon Basin, like studies carried out in other forests around the world (e.g., US, Helliker and Ehleringer 2000; Helliker and Ehleringer (2000);
435 Yakir (2003); in Beijing, China Wang et al. (2021, 2022)). Field experiments focused on the vertical distribution of $PAR_f$ radiation throughout the canopy will improve the current understanding of the individual effects of aerosols and clouds on the forest microclimate ($CL_T$ and VPD) on $\%NEE$.

### 3.6 Effects of fires on biophysical variables

Important direct interference of aerosols on environmental variables that consequently affect the photosynthetic dynamics
440 of plants is observed in Fig. 9. The attenuating effect of incident solar irradiance due to the presence of aerosols triggers

statistically significant reductions in air temperature near the forest canopy. Several mechanisms have been used to explain the increase in photosynthetic capacity by the canopy due to changes in the biophysical properties of the forest, among them, the general trend of decreasing VPD Min (2005); Yuan et al. (2019) and temperatures Koren et al. (2014); Bai et al. (2012) under cloudy or smoky skies. In the present research, reductions in temperature and VPD, are also observed (Fig. 9). The

445     impact of aerosols produced, respectively, a cooling of 3 °C and 2.5 °C in $CL_T$ and $T_{ar}$ when $f$ jumped from 1.1-1.10 to 0.66 (Fig. 9, on top panel and middle panel). These results are similar to the results found by Davidi et al. (2009). The effects of these coolings, especially in $CL_T$, can exert a large positive influence on the photosynthesis of the forest Doughty et al. (2010). Figure 9 (bottom panel) shows the relationship between the VPD and the irradiance $f$ (this time, between $SZA$ angles of 0-60°). For Freedman et al. (1998), the increase in relative humidity due to cooling induced by clouds and/or aerosols can

450     increase photosynthesis Altaratz et al. (2008), as the increase in0 humidity induces stomatal opening Collatz et al. (1991); Jing et al. (2010). In many forest locations, the reduction in $f$ produces a decrease in VPD of around 35% during the dry season. These reductions, strongly influenced by the cooling of the air, are also closely linked with the cooling of the forest canopy and the increase in the absorption capacity of $CO_2$ (%$NEE$) Doughty et al. (2010). For cloudy and/or polluted sky conditions, generally decreasing VPD behavior can influence stomata opening and intensify photosynthesis Jing et al. (2010). Studies

455     focused on the impacts of fires on the flux of water to the atmosphere deserve attention and can help to understand the role of forests in maintaining rainfall and its effects on the hydrological cycle (studies not yet carried out for most biomes in the Amazon).

     The results presented in Fig. 9, viewed as a function of the frequency distribution of the clarity index $kt$, indicate that the current patterns of aerosol loading on the studied semideciduous forest ecosystem exceed the maximum limit for the

460     which dense upland forests of central Amazônia reach the maximum amounts of carbon uptake (results not shown) Oliveira et al. (2007); Cirino et al. (2014); Doughty et al. (2010). This finding, in particular, reveals greater tolerance (resilience) of semideciduous forests to aerosol loads by fires in Mato Grosso region over the last 30 years.

     Unlike what was found here, the forests of central Amazonia, in Manaus-AM (K34), FLONA-Tapajós (K83), Santarém-PA and Ji-Paraná (RO) seem to be less tolerant to the attenuations of sunlight induced by clouds and aerosols, required for the

465     photosynthesis process. In our forest, the distribution of $kt$ is close to 0.66 for $AOD_a \gg 0.10$ Table 5. This value is 15-20% lower than values found in central Amazônia, when the $NEE$ reaches maximum negative values during the burning season ($kt \sim 0.80$). This is the threshold value at which maximum carbon absorption is observed due to cloudiness and/or aerosol load in the JBR in the Ji-Paraná JBR (south of the Amazon basin) as well as in the Cuieiras reserve at K34, in Manaus-AM. These comparisons are relevant because higher (lower) amounts of aerosols and clouds in the Amazon region can cause certain types

470     of forests to absorb even higher (lower) amounts of carbon throughout the day Gu et al. (1999); Cirino et al. (2014). The $kt$ frequency distribution patterns and their impacts on photosynthesis remain unknown for many other forest types in the Amazon and around the world. The results reported here are also consistent with calculations by Gu et al. (1999), for temperate forests in Canada, where negative maximums in $NEE$ flux occur for ranges $kt$ between 0.55– 0.60.

     The interannual variability of the relationship between the observed $AODa$, fire counts and $NEE$ could not be analyzed,

475     mainly due to the lack of a long time series of $NEE$ flux data in the region. In the central Amazon, significant variability
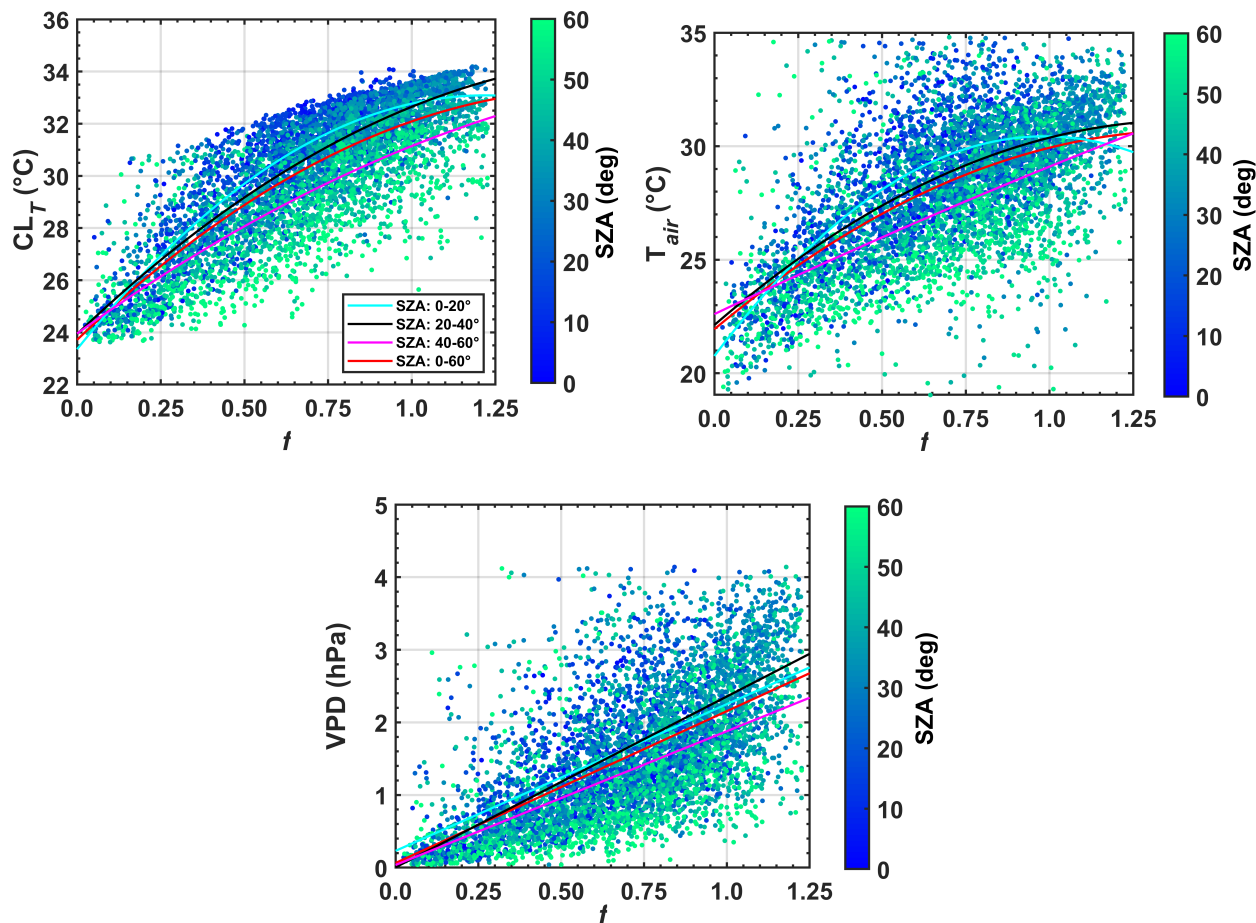
**Figure 9.** Correlation between the relative irradiance $f$ with $CL_T$ (top panel), $T_{air}$ (middle panel) and VPD (bottom panel), values calculated for $SZA$ between 0 and 60. The air temperature was measured at 42 m above the ground, in the micrometeorological tower located in the municipality of Cláudia, 50 km from Sinop-MT, using the parameterization given in Tribuzy (2005), between 2003-2004.

was observed from year to year. Higher $\%NEE$ were often found on days with high fire counts. However, water stress and nutrient availability also play an important role in the carbon uptake capacity Gatti et al. (2014); Hofhansl et al. (2016); Gatti et al. (2021); Malhi et al. (2021). Joint modifications in these variables make it extremely difficult to quantify the individual effects of aerosols and clouds on the $NEE$. Field experiments taking measurements of all these aspects will yield studies
480 with more robust and comprehensive conclusions on the ecosystem responses of Amazonian forests to external environmental disturbances such as fires.

## 4    Conclusions

The aerosol optical depth derived from the AERONET system proved to be a key variable in the elaboration of the clear sky solar irradiance model used to determine the relative irradiance $f$. The conceived model can be directed to other regions of the Amazon as long as they are within the same latitude range, where there are no $SW_i$ measurements. In this study, it was possible to separate the radiative effects of aerosols from the effects produced by clouds, combining the measurements of incident solar radiation from the AERONET system with the $AOD_a$ measurements.

The parameter $f$, allowed us to satisfactorily evaluate the radiative effects of aerosols from fires on the net absorption of carbon by the studied semideciduous forest ecosystem, absorption here represented by the $NEE$ flux. The radiative impacts on $PAR_i$ and $PAR_d$ allowed us to evaluate the impacts on the canopy light use efficiency ($LUE$), which increased by $\sim$ 1-3% under polluted conditions ($AOD_a$). The changes in incident solar radiation and $CO_2$ flux ($NEE$) could be attributed to the combined effects of aerosols emitted locally, regionally, or transported from more distant regions, considering the applied methods.

In the studied semideciduous forest ecosystem, the net carbon flux ($NEE$) increased from 20-70% when the optical depth varied from 0.1 to 5.0 (on average). This effect was attributed to an average reduction of up to 40% in the amount of total PAR radiation and also to an increase of up to 50% in the diffuse fraction of radiation ($PAR(D)_F$). This increase in $CO_2$ absorption capacity by the ecosystem is closely linked to the floristic composition of the understory and certain types of forest species adapted to low light conditions, which consists of more efficient vegetation in capturing diffused light during the photosynthesis process. The results show higher photosynthetic efficiency under smoky sky conditions; loaded with particles scattering solar radiation due to fires, but also reveal the maximum limit in the PAR radiation cuts required for the photosynthesis process. Relative irradiances $f$ less than 0.66, on average, indicate the critical point at which forest photosynthetic rates undergo drastic reductions. Irradiance values $f \sim$ of 0.22 indicate 100% interruption in the photosynthetic process.

Due to the increase in the concentration of aerosol particles from fires in the region, statistically, significant changes were also observed in meteorological (biophysical) variables such as leaf canopy temperature and VPD. Scientific findings reveal a strong influence of fire aerosols on these variables, with potentially important effects on photosynthesis and carbon absorption. The 3 and 5 °C reductions in leaf canopy and air temperature are strongly associated with a 40% reduction in $f$ and a $\sim$ 2.0 mb reduction in VPD values which induce opening stomata and contribute to the observed increase of 20-70% in the $CO_2$ absorption capacity of the forest ($\%NEE$). The individual influences or contributions of the VPD, $T_{air}$ and $CL_T$ to the ecosystem's net balance of $CO_2$, however, could not be directly quantified in this research. Indirect correlations, however, reveal statistically significant effects between the mentioned biophysical variables and the observed changes in the $NEE$ flux during the exposure of forests to fire and high values of $AOD_a$ (greater than 1.25, on average).

### 4.1    Suggestions for future work

A more comprehensive regional study of the effects mentioned here, based on other vegetation types and biomes, using vegetation maps, remote sensing estimates, meteorological data, and numerical modeling, will help to better understand how

515 the climate and ecosystem function in the Amazon are affected by natural and anthropic environmental. The reductions in the $NEE$ flux and, therefore, the reduction of the photosynthetic capacity of the plants due to the excessive increase in the concentration of BBOA aerosols and drastic reductions in the fluxes of solar radiation ($f \leq 0.22$) due to the fires in the region, constitutes an effect of notable relevance for carbon cycling in semi-deciduous forest environments in the Amazon and, therefore, an important contribution to a better understanding of this cycle in the region and the world.

520 *Data availability.* This section provides free access to data repositories that support the conclusions. Turbulent covariance data and Automatic Weather Systems, as well as selected formulas, will be available shortly on the Ameriflux website (https://ameriflux.lbl.gov) according to Vourlitis et al. (2011): "Temporal patterns of net $CO_2$ exchange for a semideciduous tropical forest in the southern Amazon Basin". Alternatively, we provide the data from this survey available through the Mendeley Data platform (https://data.mendeley.com), where we will make upgrades and possible corrections. Citation: Cirino, Glauber; Vourlitis, George; Silva, Simone; Palácios, Rafael (2022), "Brazil-
525 FluxMet-Stf", Mendeley Data, v2 DOI: 10.17632/m5h5fw872g.2. Secondary data is already in the public domain. We have listed the links to these data in the Supporting Information (Table S3)

# References

Ackerly, D. D., Thomas, W. M. W., Ferreira, C. A. C. I. D., and Pirani, J. R.: The forest-cerrado transition zone in southern Amazonia: results
of the 1985 project flora amazonica expedition to Mato Grosso, 41, 113–128, 1989.

Adachi, K., Oshima, N., Gong, Z., de Sá, S., Bateman, A. P., Martin, S. T., de Brito, J. F., Artaxo, P., Cirino, G. G., Sedlacek III, A. J., and
Buseck, P. R.: Mixing states of Amazon basin aerosol particles transported over long distances using transmission electron microscopy,
Atmospheric Chemistry and Physics, 20, 11 923–11 939, https://doi.org/10.5194/acp-20-11923-2020, 2020.

Alencar, A. A. C., Arruda, V. L. S., Silva, W. V. d., Conciani, D. E., Costa, D. P., Crusco, N., Duverger, S. G., Ferreira, N. C., Franca-Rocha,
W., Hasenack, H., Martenexen, L. F. M., Piontekowski, V. J., Ribeiro, N. V., Rosa, E. R., Rosa, M. R., dos Santos, S. M. B., Shimbo, J. Z.,
and Vélez-Martin, E.: Long-Term Landsat-Based Monthly Burned Area Dataset for the Brazilian Biomes Using Deep Learning, Remote
Sensing, 14, https://doi.org/10.3390/rs14112510, 2022.

Altaratz, O., Koren, I., and Reisin, T.: Humidity impact on the aerosol effect in warm cumulus clouds, Geophysical Research Letters, 35,
1–5, https://doi.org/10.1029/2008GL034178, 2008.

Amorim Neto, A. d. C., Satyamurty, P., and Correia, F. W.: Some observed characteristics of frontal systems in the Amazon Basin, Meteoro-
logical Applications, 22, 617–635, https://doi.org/https://doi.org/10.1002/met.1497, 2015.

Aragão, L. E., Anderson, L. O., Fonseca, M. G., Rosan, T. M., Vedovato, L. B., Wagner, F. H., Silva, C. V., Silva Junior, C. H., Arai, E.,
Aguiar, A. P., Barlow, J., Berenguer, E., Deeter, M. N., Domingues, L. G., Gatti, L., Gloor, M., Malhi, Y., Marengo, J. A., Miller, J. B.,
Phillips, O. L., and Saatchi, S.: 21st Century drought-related fires counteract the decline of Amazon deforestation carbon emissions,
Nature Communications, 9, 1–12, https://doi.org/10.1038/s41467-017-02771-y, 2018.

Araújo, A. C., Dolman, A. J., Waterloo, M. J., Gash, J. H., Kruijt, B., Zanchi, F. B., de Lange, J. M., Stoevelaar, R., Manzi, A. O., Nobre,
A. D., Lootens, R. N., and Backer, J.: The spatial variability of CO2 storage and the interpretation of eddy covariance fluxes in central
Amazonia, Agricultural and Forest Meteorology, 150, 226–237, https://doi.org/10.1016/j.agrformet.2009.11.005, 2010.

Artaxo, P., Rizzo, L. V., Brito, J. F., Barbosa, H. M., Arana, A., Sena, E. T., Cirino, G. G., Bastos, W., Martin, S. T., and Andreae, M. O.:
Atmospheric aerosols in Amazonia and land use change: From natural biogenic to biomass burning conditions, Faraday Discussions, 165,
203–235, https://doi.org/10.1039/c3fd00052d, 2013.

Artaxo, P., Mohr, C., and Pöschl, U.: Tropical and Boreal Forest – Atmosphere Interactions : A Review, 74, 24–163,
https://doi.org/10.16993/tellusb.34, 2022.

Aubinet, M.: Eddy Covariance, https://doi.org/10.1007/978-94-007-2351-1, 2012.

Aubinet, M., Chermanne, B., Vandenhaute, M., Longdoz, B., Yernaux, M., and Laitat, E.: Long term carbon dioxide exchange above a mixed
forest in the Belgian Ardennes, Agricultural and Forest Meteorology, 108, 293–315, https://doi.org/10.1016/S0168-1923(01)00244-1,
2001.

Avitabile, V., Herold, M., Heuvelink, G. B., Lewis, S. L., Phillips, O. L., Asner, G. P., Armston, J., Ashton, P. S., Banin, L., Bayol, N.,
Berry, N. J., Boeckx, P., de Jong, B. H., Devries, B., Girardin, C. A., Kearsley, E., Lindsell, J. A., Lopez-Gonzalez, G., Lucas, R., Malhi,
Y., Morel, A., Mitchard, E. T., Nagy, L., Qie, L., Quinones, M. J., Ryan, C. M., Ferry, S. J., Sunderland, T., Laurin, G. V., Gatti, R. C.,
Valentini, R., Verbeeck, H., Wijaya, A., and Willcock, S.: An integrated pan-tropical biomass map using multiple reference datasets,
Global Change Biology, 22, 1406–1420, https://doi.org/10.1111/gcb.13139, 2016.

Bai, Y., Wang, J., Zhang, B., Zhang, Z., and Liang, J.: Comparing the impact of cloudiness on carbon dioxide exchange in a grassland and a
maize cropland in northwestern China, Ecological Research, 27, 615–623, https://doi.org/10.1007/s11284-012-0930-z, 2012.

26

Balch, J. K., Brando, P. M., Nepstad, D. C., Coe, M. T., Silvério, D., Massad, T. J., Davidson, E. A., Lefebvre, P., Oliveira-Santos, C., Rocha, W., Cury, R. T., Parsons, A., and Carvalho, K. S.: The Susceptibility of Southeastern Amazon Forests to Fire: Insights from a Large-Scale Burn Experiment, BioScience, 65, 893–905, https://doi.org/10.1093/biosci/biv106, 2015.

Beer, C., Reichstein, M., Tomelleri, E., Ciais, P., Jung, M., Carvalhais, N., Rödenbeck, C., Arain, M. A., Baldocchi, D., Bonan, G. B., Bondeau, A., Cescatti, A., Lasslop, G., Lindroth, A., Lomas, M., Luyssaert, S., Margolis, H., Oleson, K. W., Roupsard, O., Veenendaal, E., Viovy, N., Williams, C., Woodward, F. I., and Papale, D.: Terrestrial gross carbon dioxide uptake: Global distribution and covariation with climate, Science, 329, 834–838, https://doi.org/10.1126/science.1184984, 2010.

Bian, H., Lee, E., Koster, R. D., Barahona, D., Chin, M., Colarco, P. R., Darmenov, A., Mahanama, S., Manyin, M., Norris, P., Shilling, J., Yu, H., and Zeng, F.: The response of the Amazon ecosystem to the photosynthetically active radiation fields: Integrating impacts of biomass burning aerosol and clouds in the NASA GEOS Earth system model, Atmospheric Chemistry and Physics, 21, 14 177–14 197, https://doi.org/10.5194/acp-21-14177-2021, 2021.

Booth, B. B., Jones, C. D., Collins, M., Totterdell, I. J., Cox, P. M., Sitch, S., Huntingford, C., Betts, R. A., Harris, G. R., and Lloyd, J.: High sensitivity of future global warming to land carbon cycle processes, Environmental Research Letters, 7, https://doi.org/10.1088/1748-9326/7/2/024002, 2012.

Braghiere, Kerches Renato, Akemi Yamasoe, M., Manuel Évora do RosáRio, N., Ribeiro Da Rocha, H., De Souza Nogueira, J., and Carioca de AraÚJo, A.: Characterization of the radiative impact of aerosols on CO2 and energy fluxes in the Amazon deforestation arch using artificial neural networks, Atmospheric Chemistry and Physics, 20, 3439–3458, https://doi.org/10.5194/acp-20-3439-2020, 2020.

Brienen, R. J., Phillips, O. L., Feldpausch, T. R., Gloor, E., Baker, T. R., Lloyd, J., Lopez-Gonzalez, G., Monteagudo-Mendoza, A., Malhi, Y., Lewis, S. L., Vásquez Martinez, R., Alexiades, M., Álvarez Dávila, E., Alvarez-Loayza, P., Andrade, A., Aragaõ, L. E., Araujo-Murakami, A., Arets, E. J., Arroyo, L., Aymard C., G. A., Bánki, O. S., Baraloto, C., Barroso, J., Bonal, D., Boot, R. G., Camargo, J. L., Castilho, C. V., Chama, V., Chao, K. J., Chave, J., Comiskey, J. A., Cornejo Valverde, F., Da Costa, L., De Oliveira, E. A., Di Fiore, A., Erwin, T. L., Fauset, S., Forsthofer, M., Galbraith, D. R., Grahame, E. S., Groot, N., Hérault, B., Higuchi, N., Honorio Coronado, E. N., Keeling, H., Killeen, T. J., Laurance, W. F., Laurance, S., Licona, J., Magnussen, W. E., Marimon, B. S., Marimon-Junior, B. H., Mendoza, C., Neill, D. A., Nogueira, E. M., Núñez, P., Pallqui Camacho, N. C., Parada, A., Pardo-Molina, G., Peacock, J., Penã-Claros, M., Pickavance, G. C., Pitman, N. C., Poorter, L., Prieto, A., Quesada, C. A., Ramírez, F., Ramírez-Angulo, H., Restrepo, Z., Roopsind, A., Rudas, A., Salomaõ, R. P., Schwarz, M., Silva, N., Silva-Espejo, J. E., Silveira, M., Stropp, J., Talbot, J., Ter Steege, H., Teran-Aguilar, J., Terborgh, J., Thomas-Caesar, R., Toledo, M., Torello-Raventos, M., Umetsu, R. K., Van Der Heijden, G. M., Van Der Hout, P., Guimarães Vieira, I. C., Vieira, S. A., Vilanova, E., Vos, V. A., and Zagt, R. J.: Long-term decline of the Amazon carbon sink, Nature, 519, 344–348, https://doi.org/10.1038/nature14283, 2015.

Burba, G.: Eddy Covariance Method for Scientific, Industrial, Agricultural and Regulatory Applications: A Field Book on Measuring Ecosystem Gas Exchange and Areal Emission Rates, https://doi.org/10.13140/RG.2.1.4247.8561, 2013.

Carswell, F. E., Costa, A. L., Palheta, M., Malhi, Y., Meir, P., Costa, J. d. P. R., Ruivo, M. d. L., Leal, L. d. S. M., Costa, J. M. N., Clement, R. J., and Grace, J.: Seasonality in CO2 and H2O flux at an eastern Amazonian rain forest, Journal of Geophysical Research: Atmospheres, 107, LBA 43–1–LBA 43–16, https://doi.org/https://doi.org/10.1029/2000JD000284, 2002.

Cirino, G., Brito, J., Barbosa, H. M., Rizzo, L. V., Tunved, P., de Sá, S. S., Jimenez, J. L., Palm, B. B., Carbone, S., Lavric, J. V., Souza, R. A., Wolff, S., Walter, D., Tota, J., Oliveira, M. B., Martin, S. T., and Artaxo, P.: Observations of Manaus urban plume evolution and interaction with biogenic emissions in GoAmazon 2014/5, Atmospheric Environment, 191, 513–524, https://doi.org/10.1016/j.atmosenv.2018.08.031, 2018.

27

Cirino, G. G., Souza, R. A., Adams, D. K., and Artaxo, P.: The effect of atmospheric aerosol particles and clouds on net ecosystem exchange in the Amazon, Atmospheric Chemistry and Physics, 14, 6523–6543, https://doi.org/10.5194/acp-14-6523-2014, 2014.

615 Collatz, G. J., Ball, J. T., Grivet, C., and Berry, J. A.: Physiological and environmental regulation of stomatal conductance, photosynthesis and transpiration: a model that includes a laminar boundary layer, Agricultural and Forest Meteorology, 54, 107–136, https://doi.org/10.1016/0168-1923(91)90002-8, 1991.

Davidi, A., Koren, I., and Remer, L.: Direct measurements of the effect of biomass burning over the Amazon on the atmospheric temperature profile, Atmospheric Chemistry and Physics, 9, 8211–8221, https://doi.org/10.5194/acp-9-8211-2009, 2009.

620 de Magalhães, N., Evangelista, H., Condom, T., Rabatel, A., and Ginot, P.: Amazonian Biomass Burning Enhances Tropical Andean Glaciers Melting, Scientific Reports, 9, 1–12, https://doi.org/10.1038/s41598-019-53284-1, 2019.

de Sá, S. S., Rizzo, L. V., Palm, B. B., Campuzano-Jost, P., Day, D. A., Yee, L. D., Wernis, R., Isaacman-VanWertz, G., Brito, J., Carbone, S., Liu, Y. J., Sedlacek, A., Springston, S., Goldstein, A. H., Barbosa, H. M. J., Alexander, M. L., Artaxo, P., Jimenez, J. L., and Martin, S. T.: Contributions of biomass-burning, urban, and biogenic emissions to the concentrations and light-absorbing properties of particulate

625 matter in central Amazonia during the dry season, Atmospheric Chemistry and Physics, 19, 7973–8001, https://doi.org/10.5194/acp-19-7973-2019, 2019.

Doughty, C. E., Flanner, M. G., and Goulden, M. L.: Effect of smoke on subcanopy shaded light, canopy temperature, and carbon dioxide uptake in an Amazon rainforest, Global Biogeochemical Cycles, 24, 1–10, https://doi.org/10.1029/2009GB003670, 2010.

Doughty, C. E., Metcalfe, D. B., Girardin, C. A., Amézquita, F. F., Cabrera, D. G., Huasco, W. H., Silva-Espejo, J. E., Araujo-Murakami, A.,

630 Da Costa, M. C., Rocha, W., Feldpausch, T. R., Mendoza, A. L., Da Costa, A. C., Meir, P., Phillips, O. L., and Malhi, Y.: Drought impact on forest carbon dynamics and fluxes in Amazonia, Nature, 519, 78–82, https://doi.org/10.1038/nature14213, 2015.

Finnigan, J.: The storage term in eddy flux calculations, Agricultural and Forest Meteorology, 136, 108–113, https://doi.org/10.1016/j.agrformet.2004.12.010, 2006.

Foken, T.: Micrometeorology, Springer Berlin Heidelberg, https://doi.org/10.1007/978-3-540-74666-9, 2008.

635 Freedman, J., Fitzjarrald, D., Moore, K., and Sakai, R.: Boundary layer cloud climatology and enhanced forest-atmosphere exchange, in: Preprints of 23rd Conference on Agricultural and Forest Meteorology, pp. 41–44, 1998.

Fu, Z., Gerken, T., Bromley, G., Araújo, A., Bonal, D., Burban, B., Ficklin, D., Fuentes, J. D., Goulden, M., Hirano, T., Kosugi, Y., Liddell, M., Nicolini, G., Niu, S., Roupsard, O., Stefani, P., Mi, C., Tofte, Z., Xiao, J., Valentini, R., Wolf, S., and Stoy, P. C.: The surface-atmosphere exchange of carbon dioxide in tropical rainforests: Sensitivity to environmental drivers and flux measurement methodology,

640 Agricultural and Forest Meteorology, 263, 292–307, https://doi.org/10.1016/j.agrformet.2018.09.001, 2018.

Gao, Y.: Atmospheric Aerosols Elevated Ecosystem Productivity of a Poplar Plantation in Beijing, 2 China, 2020.

Gates, D. M.: Biophysical Ecology, 1980.

Gatti, L. V., Gloor, M., Miller, J. B., Doughty, C. E., Malhi, Y., Domingues, L. G., Basso, L. S., Martinewski, A., Correia, C. S., Borges, V. F., Freitas, S., Braz, R., Anderson, L. O., Rocha, H., Grace, J., Phillips, O. L., and Lloyd, J.: Drought sensitivity of Amazonian carbon

645 balance revealed by atmospheric measurements, Nature, 506, 76–80, https://doi.org/10.1038/nature12957, 2014.

Gatti, L. V., Basso, L. S., Miller, J. B., Gloor, M., Gatti Domingues, L., Cassol, H. L., Tejada, G., Aragão, L. E., Nobre, C., Peters, W., Marani, L., Arai, E., Sanches, A. H., Corrêa, S. M., Anderson, L., Von Randow, C., Correia, C. S., Crispim, S. P., and Neves, R. A.: Amazonia as a carbon source linked to deforestation and climate change, Nature, 595, 388–393, https://doi.org/10.1038/s41586-021-03629-6, 2021.

Grace, J., Malhi, Y., Lloyd, J., McIntyre, J., Miranda, A. C., Meir, P., and Miranda, H. S.: The use of eddy covariance to infer the net carbon

650 dioxide uptake of Brazilian rain forest, Global Change Biology, 2, 209–217, https://doi.org/10.1111/j.1365-2486.1996.tb00073.x, 1996.

Gu, L., Fuentes, J. D., Shugart, H. H., Staebler, R. M., and Black, T. A.: Responses of net ecosystem exchanges of carbon dioxide to changes in cloudiness: Results from two North American deciduous forests, Journal of Geophysical Research Atmospheres, 104, 31 421–31 434, https://doi.org/10.1029/1999JD901068, 1999.

Gu, L., Fuentes, J. D., Garstang, M., Silva, J. T. D., Heitz, R., Sigler, J., and Shugart, H. H.: Cloud modulation of surface solar irradiance at a pasture site in Southern Brazil, Agricultural and Forest Meteorology, 106, 117–129, https://doi.org/10.1016/S0168-1923(00)00209-4, 2001.

Helliker, B. R. and Ehleringer, J. R.: Establishing a grassland signature in veins: [18]O in the leaf water of $C_3$ and $C_4$ grasses, Proceedings of the National Academy of Sciences, 97, 7894–7898, https://doi.org/10.1073/pnas.97.14.7894, 2000.

Hofhansl, F., Andersen, K. M., Fleischer, K., Fuchslueger, L., Rammig, A., Schaap, K. J., Valverde-Barrantes, O. J., and Lapola, D. M.: Amazon forest ecosystem responses to elevated atmospheric Co2 and alterations in nutrient availability: Filling the gaps with model-experiment integration, Frontiers in Earth Science, 4, 1–9, https://doi.org/10.3389/feart.2016.00019, 2016.

Holben, B. N., Eck, T. F., Slutsker, I., Tanré, D., Buis, J. P., Setzer, A., Vermote, E., Reagan, J. A., Kaufman, Y. J., Nakajima, T., Lavenu, F., Jankowiak, I., and Smirnov, A.: AERONET - A federated instrument network and data archive for aerosol characterization, Remote Sensing of Environment, 66, 1–16, https://doi.org/10.1016/S0034-4257(98)00031-5, 1998.

Hollinger, D. Y. and Richardson, A. D.: Uncertainty in eddy covariance measurements and its application to physiological models, pp. 873–885, 2005.

Huntingford, C., Zelazowski, P., Galbraith, D., Mercado, L. M., Sitch, S., Fisher, R., Lomas, M., Walker, A. P., Jones, C. D., Booth, B. B., Malhi, Y., Hemming, D., Kay, G., Good, P., Lewis, S. L., Phillips, O. L., Atkin, O. K., Lloyd, J., Gloor, E., Zaragoza-Castells, J., Meir, P., Betts, R., Harris, P. P., Nobre, C., Marengo, J., and Cox, P. M.: Simulated resilience of tropical rainforests to CO2 -induced climate change, Nature Geoscience, 6, 268–273, https://doi.org/10.1038/ngeo1741, 2013.

Jing, X., Huang, J., Wang, G., Higuchi, K., Bi, J., Sun, Y., Yu, H., and Wang, T.: The effects of clouds and aerosols on net ecosystem CO 2 exchange over semi-arid Loess Plateau of Northwest China, Atmospheric Chemistry and Physics, 10, 8205–8218, https://doi.org/10.5194/acp-10-8205-2010, 2010.

Kanniah, K. D., Beringer, J., North, P., and Hutley, L.: Control of atmospheric particles on diffuse radiation and terrestrial plant productivity: A review, Progress in Physical Geography, 36, 209–237, https://doi.org/10.1177/0309133311434244, 2012.

Koren, I., Dagan, G., and Altaratz, O.: From aerosol-limited to invigoration of warm convective clouds, Science, 344, 1143–1146, https://doi.org/10.1126/science.1252595, 2014.

Levy, R. C., Mattoo, S., Munchak, L. A., Remer, L. A., Sayer, A. M., Patadia, F., and Hsu, N. C.: The Collection 6 MODIS aerosol products over land and ocean, Atmospheric Measurement Techniques, 6, 2989–3034, https://doi.org/10.5194/amt-6-2989-2013, 2013.

Lorenzi, H.: Arvores , brasileiras, São Paulo, 2000.

Lorenzi, H.: Arvores , brasileiras, Sao Paulo, 2002.

Malavelle, F. F., Haywood, J. M., Mercado, L. M., Folberth, G. A., Bellouin, N., Sitch, S., and Artaxo, P.: Studying the impact of biomass burning aerosol radiative and climate effects on the Amazon rainforest productivity with an Earth system model, Atmospheric Chemistry and Physics, 19, 1301–1326, https://doi.org/10.5194/acp-19-1301-2019, 2019.

Malhi, Y., Melack, J., Gatti, L. V., Ometto, J. P., Kesselmeier, J., Wolff, S., Aragão, L. E. O., Costa, M. H., Saleska, S. R., Pangala, S., Basso, L. S., Rizzo, L., de Araújo, A. C., Restrepo-Coupe, N., and Silva Junior, C. H. L.: Chapter 6: Biogeochemical Cycles in the Amazon, https://doi.org/10.55161/takr3454, 2021.

Martin, S. T., Andreae, M. O., Althausen, D., Artaxo, P., Baars, H., Borrmann, S., Chen, Q., Farmer, D. K., Guenther, A., Gunthe, S. S.,
690     Jimenez, J. L., Karl, T., Longo, K., Manzi, A., Müller, T., Pauliquevis, T., Petters, M. D., Prenni, A. J., Pöschl, U., Rizzo, L. V., Schneider,
    J., Smith, J. N., Swietlicki, E., Tota, J., Wang, J., Wiedensohler, A., and Zorn, S. R.: An overview of the Amazonian Aerosol Character-
    ization Experiment 2008 (AMAZE-08), Atmospheric Chemistry and Physics, 10, 11 415–11 438, https://doi.org/10.5194/acp-10-11415-
    2010, 2010a.

Martin, S. T., Andreae, M. O., Artaxo, P., Baumgardner, D., Chen, Q., Goldstein, A. H., Guenther, A., Heald, C. L., Mayol-Bracero, O. L.,
695     McMurry, P. H., Pauliquevis, T., Pschl, U., Prather, K. A., Roberts, G. C., Saleska, S. R., Silva Dias, M. A., Spracklen, D. V., Swietlicki, E.,
    and Trebs, I.: Sources and properties of Amazonian aerosol particles, Reviews of Geophysics, 48, https://doi.org/10.1029/2008RG000280,
    2010b.

MATLAB: version 9.8.8.748 (R2013a), The MathWorks Inc., Natick, Massachusetts, 2013.

Mercado, L. M., Bellouin, N., Sitch, S., Boucher, O., Huntingford, C., Wild, M., and Cox, P. M.: Impact of changes in diffuse radiation on
700     the global land carbon sink, Nature, 458, 1014–1017, https://doi.org/10.1038/nature07949, 2009.

Meyers, T. P. and Dale, R. F.: Predicting daily insolation with hourly cloud height and coverage., https://doi.org/10.1175/1520-
    0450(1983)022<0537:PDIWHC>2.0.CO;2, 1983.

Min, Q.: Impacts of aerosols and clouds on forest-atmosphere carbon exchange, Journal of Geophysical Research: Atmospheres, 110,
    https://doi.org/https://doi.org/10.1029/2004JD004858, 2005.

705 Moncrieff, J. B., Massheder, J. M., De Bruin, H., Elbers, J., Friborg, T., Heusinkveld, B., Kabat, P., Scott, S., Soegaard, H., and Verhoef,
    A.: A system to measure surface fluxes of momentum, sensible heat, water vapour and carbon dioxide, Journal of Hydrology, 188-189,
    589–611, https://doi.org/10.1016/S0022-1694(96)03194-0, 1997.

Montagnani, L., Grünwald, T., Kowalski, A., Mammarella, I., Merbold, L., Metzger, S., Sedlák, P., and Siebicke, L.: Estimating the storage
    term in eddy covariance measurements: The ICOS methodology, International Agrophysics, 32, 551–567, https://doi.org/10.1515/intag-
710     2017-0037, 2018.

Moreira, D. S., Freitas, S. R., Bonatti, J. P., Mercado, L. M., É. Rosário, N. M., Longo, K. M., Miller, J. B., Gloor, M., and Gatti, L. V.:
    Coupling between the JULES land-surface scheme and the CCATT-BRAMS atmospheric chemistry model (JULES-CCATT-BRAMS1.0):
    Applications to numerical weather forecasting and the CO2 budget in South America, Geoscientific Model Development, 6, 1243–1259,
    https://doi.org/10.5194/gmd-6-1243-2013, 2013.

715 Moreira, D. S., Longo, K. M., Freitas, S. R., Yamasoe, M. A., Mercado, L. M., Rosário, N. E., Gloor, E., Viana, R. S., Miller, J. B., Gatti,
    L. V., Wiedemann, K. T., Domingues, L. K., and Correia, C. C.: Modeling the radiative effects of biomass burning aerosols on carbon
    fluxes in the Amazon region, Atmospheric Chemistry and Physics, 17, 14 785–14 810, https://doi.org/10.5194/acp-17-14785-2017, 2017.

Morgan, W. T., Darbyshire, E., Spracklen, D. V., Artaxo, P., and Coe, H.: Non-deforestation drivers of fires are increasingly important sources
    of aerosol and carbon dioxide emissions across Amazonia, Scientific Reports, 9, 1–15, https://doi.org/10.1038/s41598-019-53112-6, 2019.

720 Murphy, P. G. and Lugo, A. E.: Ecology of tropical dry forest., Annual review of ecology and systematics. Vol. 17, pp. 67–88,
    https://doi.org/10.1146/annurev.es.17.110186.000435, 1986.

Nagy, L., Artaxo, P., and Forsberg, B. R.: Interactions Between Biosphere, Atmosphere, and Human Land Use in the Amazon Basin: An
    Introduction, https://doi.org/10.1007/978-3-662-49902-3_1, 2016.

Nagy, R. C., Porder, S., Brando, P., Davidson, E. A., Figueira, A. M. e. S., Neill, C., Riskin, S., and Trumbore, S.: Soil Carbon Dy-
725     namics in Soybean Cropland and Forests in Mato Grosso, Brazil, Journal of Geophysical Research: Biogeosciences, 123, 18–31,
    https://doi.org/https://doi.org/10.1002/2017JG004269, 2018.

Nepstad, D., McGrath, D., Stickler, C., Alencar, A., Azevedo, A., Swette, B., Bezerra, T., DiGiano, M., Shimada, J., Da Motta, R. S., Armijo, E., Castello, L., Brando, P., Hansen, M. C., McGrath-Horn, M., Carvalho, O., and Hess, L.: Slowing Amazon deforestation through public policy and interventions in beef and soy supply chains, Science, 344, 1118–1123, https://doi.org/10.1126/science.1248525, 2014.

730 Niyogi, D., Chang, H. I., Saxena, V. K., Holt, T., Alapaty, K., Booker, F., Chen, F., Davis, K. J., Holben, B., Matsui, T., Meyers, T., Oechel, W. C., Pielke, R. A., Wells, R., Wilson, K., and Xue, Y.: Direct observations of the effects of aerosol loading on net ecosystem CO 2 exchanges over different landscapes, Geophysical Research Letters, 31, 1–5, https://doi.org/10.1029/2004GL020915, 2004.

Nogueira, E. M., Nelson, B. W., Fearnside, P. M., França, M. B., and de Oliveira, Á. C. A.: Tree height in Brazil's 'arc of defor-estation': Shorter trees in south and southwest Amazonia imply lower biomass, Forest Ecology and Management, 255, 2963–2972,
735 https://doi.org/10.1016/j.foreco.2008.02.002, 2008.

Oliveira, P. H., Artaxo, P., Pires, C., De Lucca, S., Procópio, A., Holben, B., Schafer, J., Cardoso, L. F., Wofsy, S. C., and Rocha, H. R.: The effects of biomass burning aerosols and clouds on the CO2 flux in Amazonia, Tellus, Series B: Chemical and Physical Meteorology, 59, 338–349, https://doi.org/10.1111/j.1600-0889.2007.00270.x, 2007.

Oliveira-Filho AT, R. J. and Oliveira: The Cerrados of Brazil, vol. 20, Nova York, https://doi.org/10.1258/ijsa.2009.009019, 2002.

740 Pan, Y.: A large and persistent carbon sink in the world's forests, Science, 333, 988–993, 2011.

Prado, D. E. and Gibbs, P. E.: Patterns of Species Distributions in the Dry Seasonal Forests of South America, Annals of the Missouri Botanical Garden, 80, 902, https://doi.org/10.2307/2399937, 1993.

Procopio, A. S., Artaxo, P., Kaufman, Y. J., Remer, L. A., Schafer, J. S., and Holben, B. N.: Multiyear analysis of amazonian biomass burning smoke radiative forcing of climate, Geophysical Research Letters, 31, 1–4, https://doi.org/10.1029/2003GL018646, 2004.

745 Rap, A.: Fires increase Amazon forest productivity, Geophysical Research Letters, pp. 4654–4662, https://doi.org/10.1002/2015GL063719.Received, 2015.

Rap, A., Scott, C. E., Reddington, C. L., Mercado, L., Ellis, R. J., Garraway, S., Evans, M. J., Beerling, D. J., MacKenzie, A. R., Hewitt, C. N., and Spracklen, D. V.: Enhanced global primary production by biogenic aerosol via diffuse radiation fertilization, Nature Geoscience, 11, 640–644, https://doi.org/10.1038/s41561-018-0208-3, 2018.

750 Ratter, J. A., Askew, G. P., Montgomery, R. F., and Gifford, D. R.: Observations on the vegetation of northeastern Mato Grosso II. Forests and soils of the Rio Suiá–Missu area., Proceedings of the Royal Society of London. Series B, Containing papers of a Biological character. Royal Society (Great Britain), 203, 191–208, https://doi.org/10.1098/rspb.1978.0100, 1978.

Reindl, D., Beckman, W., and Duffie, J.: Diffuse fraction correlations, Solar Energy, 45, 1–7, https://doi.org/https://doi.org/10.1016/0038-092X(90)90060-P, 1990.

755 Remer, L. A., Kaufman, Y. J., Tanré, D., Mattoo, S., Chu, D. A., Martins, J. V., Li, R. R., Ichoku, C., Levy, R. C., Kleidman, R. G., Eck, T. F., Vermote, E., and Holben, B. N.: The MODIS aerosol algorithm, products, and validation, Journal of the Atmospheric Sciences, 62, 947–973, https://doi.org/10.1175/JAS3385.1, 2005.

Remer, L. A., Mattoo, S., Levy, R. C., and Munchak, L. A.: MODIS 3 km aerosol product: Algorithm and global perspective, Atmospheric Measurement Techniques, 6, 1829–1844, https://doi.org/10.5194/amt-6-1829-2013, 2013.

760 Saatchi, S. S., Harris, N. L., Brown, S., Lefsky, M., Mitchard, E. T., Salas, W., Zutta, B. R., Buermann, W., Lewis, S. L., Hagen, S., Petrova, S., White, L., Silman, M., and Morel, A.: Benchmark map of forest carbon stocks in tropical regions across three continents, Proceedings of the National Academy of Sciences of the United States of America, 108, 9899–9904, https://doi.org/10.1073/pnas.1019576108, 2011.

Saraiva, I., Silva Dias, M. A., Morales, C. A., and Saraiva, J. M.: Regional variability of rain clouds in the amazon basin as seen by a network of weather radars, Journal of Applied Meteorology and Climatology, 55, 2657–2675, https://doi.org/10.1175/JAMC-D-15-0183.1, 2016.

765   Schafer, J. S., Eck, T. F., Holben, B. N., Artaxo, P., Yamasoe, M. A., and Procopio, A. S.: Observed reductions of total solar ir-
radiance by biomass-burning aerosols in the Brazilian Amazon and Zambian Savanna, Geophysical Research Letters, 29, 2–5,
https://doi.org/10.1029/2001GL014309, 2002a.

Schafer, J. S., Holben, B. N., Eck, T. F., Yamasoe, M. A., and Artaxo, P.: Atmospheric effects on insolation in the Brazilian Amazon: Observed
modification of solar radiation by clouds and smoke and derived single scattering albedo of fire aerosols, Journal of Geophysical Research:
770   Atmospheres, 107, LBA 41–1–LBA 41–15, https://doi.org/10.1029/2001JD000428, 2002b.

Schafer, J. S., Eck, T. F., Holben, B. N., Artaxo, P., and Duarte, A. F.: Characterization of the optical properties of atmospheric aerosols
in Amazônia from long-term AERONET monitoring (1993-1995 and 1999-2006), Journal of Geophysical Research Atmospheres, 113,
1–16, https://doi.org/10.1029/2007JD009319, 2008.

Schuepp, P. H., Leclerc, M. Y., MacPherson, J. I., and Desjardins, R. L.: Footprint prediction of scalar fluxes from analytical solutions of the
775   diffusion equation, Boundary-Layer Meteorology, 50, 355–373, https://doi.org/10.1007/BF00120530, 1990.

Shilling, J. E., Pekour, M. S., Fortner, E. C., Artaxo, P., de Sá, S., Hubbe, J. M., Longo, K. M., Machado, L. A. T., Martin, S. T., Springston,
S. R., Tomlinson, J., and Wang, J.: Aircraft observations of the chemical composition and aging of aerosol in the Manaus urban plume
during GoAmazon 2014/5, Atmospheric Chemistry and Physics, 18, 10 773–10 797, https://doi.org/10.5194/acp-18-10773-2018, 2018.

Silva, C. V., Aragão, L. E., Young, P. J., Espirito-Santo, F., Berenguer, E., Anderson, L. O., Brasil, I., Pontes-Lopes, A., Ferreira, J., Withey,
780   K., França, F., Graça, P. M., Kirsten, L., Xaud, H., Salimon, C., Scaranello, M. A., Castro, B., Seixas, M., Farias, R., and Barlow, J.: Esti-
mating the multi-decadal carbon deficit of burned Amazonian forests, Environmental Research Letters, 15, https://doi.org/10.1088/1748-
9326/abb62c, 2020.

Spitters, C. J., Toussaint, H. A., and Goudriaan, J.: Separating the diffuse and direct component of global radiation and its implications
for modeling canopy photosynthesis Part I. Components of incoming radiation, Agricultural and Forest Meteorology, 38, 217–229,
785   https://doi.org/10.1016/0168-1923(86)90060-2, 1986.

Tribuzy, E. S.: Canopy leaf temperature variations and their effect on the CO2 assimilation rate in Central Amazonia (in Portuguese), Doctoral
thesis, p. 102, 2005.

von Randow, C., Manzi, A. O., Kruijt, B., de Oliveira, P. J., Zanchi, F. B., Silva, R. L., Hodnett, M. G., Gash, J. H., Elbers, J. A., Waterloo,
M. J., Cardoso, F. L., and Kabat, P.: Comparative measurements and seasonal variations in energy and carbon exchange over forest and
790   pasture in South West Amazonia, Theoretical and Applied Climatology, 78, 5–26, https://doi.org/10.1007/s00704-004-0041-z, 2004.

Vourlitis, G. L., Priante Filho, N., Hayashi, M. M., Nogueira, J. D. S., Caseiro, F. T., and Holanda Campelo, J.: Seasonal variations
in the net ecosystem CO2 exchange of a mature Amazonian transitional tropical forest (cerradão), Functional Ecology, 15, 388–395,
https://doi.org/10.1046/j.1365-2435.2001.00535.x, 2001.

Vourlitis, G. L., Priante Filho, N., Hayashi, M. M., Nogueira, J. D. S., Caseiro, F. T., and Campelo, J. H.: Seasonal variations
795   in the evapotranspiration of a transitional tropical forest of Mato Grosso, Brazil, Water Resources Research, 38, 30–1–30–11,
https://doi.org/10.1029/2000wr000122, 2002.

Vourlitis, G. L., De Almeida Lobo, F., Zeilhofer, P., and De Souza Nogueira, J.: Temporal patterns of net CO2 exchange for
a tropical semideciduous forest of the southern Amazon Basin, Journal of Geophysical Research: Biogeosciences, 116, 1–15,
https://doi.org/10.1029/2010JG001524, 2011.

800   Wang, X., Wang, C., Wu, J., Miao, G., Chen, M., Chen, S., Wang, S., Guo, Z., Wang, Z., Wang, B., Li, J., Zhao, Y., Wu, X., Zhao, C., Lin,
W., Zhang, Y., and Liu, L.: Intermediate Aerosol Loading Enhances Photosynthetic Activity of Croplands, Geophysical Research Letters,
48, e2020GL091 893, https://doi.org/https://doi.org/10.1029/2020GL091893, e2020GL091893 2020GL091893, 2021.

Wang, Z., Wang, C., Wang, X., Wang, B., Wu, J., and Liu, L.: Aerosol pollution alters the diurnal dynamics of sun and shade leaf photosynthesis through different mechanisms, Plant, Cell & Environment, 45, 2943–2953, https://doi.org/https://doi.org/10.1111/pce.14411, 2022.

805

Yakir, D.: 4.07 - The Stable Isotopic Composition of Atmospheric CO2, in: Treatise on Geochemistry, edited by Holland, H. D. and Turekian, K. K., pp. 175–212, Pergamon, Oxford, https://doi.org/https://doi.org/10.1016/B0-08-043751-6/04038-X, 2003.

Yamasoe, M. A., Randow, C. V., Manzi, A. O., Schafer, J. S., Eck, T. F., and Holben, B. N.: Effect of smoke and clouds on the transmissivity of photosynthetically active radiation inside the canopy., pp. 1645–1656, 2006.

810

Yuan, W., Zheng, Y., Piao, S., Ciais, P., Lombardozzi, D., Wang, Y., Ryu, Y., Chen, G., Dong, W., Hu, Z., Jain, A. K., Jiang, C., Kato, E., Li, S., Lienert, S., Liu, S., Nabel, J. E., Qin, Z., Quine, T., Sitch, S., Smith, W. K., Wang, F., Wu, C., Xiao, Z., and Yang, S.: Increased atmospheric vapor pressure deficit reduces global vegetation growth, Science Advances, 5, 1–13, https://doi.org/10.1126/sciadv.aax1396, 2019.

Zhang, M., Yu, G. R., Zhang, L. M., Sun, X. M., Wen, X. F., Han, S. J., and Yan, J. H.: Impact of cloudiness on net ecosystem exchange

815

of carbon dioxide in different types of forest ecosystems in China, Biogeosciences, 7, 711–722, https://doi.org/10.5194/bg-7-711-2010, 2010.